https://ntrs.nasa.gov/search.jsp?R=19680026342 2020-03-12T06:49:20+00:00Z

Report No. 03-68-35

Final Report

for

DEVELOPMENT AND FABRICATION OF LITHIUM-DIFFUSED SILICON SOLAR CELLS

(August 18, 1966 through January 31, 1968)

Contract No. NAS 5-10274

GPO PRICE $ _____

CSFTI PRICE(S) $ _____

Hard copy (HC) _

Microfiche (MF) _

ff 653 July 65

Prepared by

D. L. Kendall
R. A. Vineyard

TEXAS INSTRUMENTS
INCORPORATED
POST OFFICE BOX 5012 • DALLAS, TEXAS 75222

OCT 1968
RECEIVED
NASA STI FACILITY
INPUT BRANCH

for

Goddard Space Flight Center
Greenbelt, Maryland

N68-35814
(ACCESSION NUMBER)
46
(PAGES)
CR-97077
(NASA CR OR TMX OR AD NUMBER)
(THRU)
1
(CODE)
03
(CATEGORY)
FACILITY FORM 602

Report No. 03-68-35

Final Report

for

DEVELOPMENT AND FABRICATION OF LITHIUM-DIFFUSED SILICON SOLAR CELLS

(August 18, 1966 through January 31, 1968)

Contract No. NAS 5-10274

Prepared by

D. L. Kendall
R. A. Vineyard

TEXAS INSTRUMENTS
INCORPORATED
POST OFFICE BOX 5012 • DALLAS, TEXAS 75222

for

Goddard Space Flight Center
Greenbelt, Maryland

PRECEDING PAGE BLANK NOT FILMED.

TABLE OF CONTENTS

PRECEDING PAGE BLANK NOT FILMED.

LIST OF ILLUSTRATIONS

PRECEDING PAGE BLANK NOT FILMED.

LIST OF TABLES

SECTION I

INTRODUCTION

A. OBJECTIVE

The objective of this contract is to develop lithium-diffused P-on-N silicon solar cells of high conversion efficiency which display improved resistance to the effects of space radiation. The work is based on an observation of Wysocki[1] that solar cells made with lithium-doped silicon demonstrated spontaneous annealing at room temperature after being damaged with high-energy electrons. The program involves the fabrication of experimental lots of silicon solar cells in which the basic parameters are varied, including base resistivity, crystal type, oxygen content, dislocation density, and lithium doping.

B. SCOPE OF WORK

The program has involved the fabrication of a large number of experimental lots of silicon solar cells. Cells have been fabricated from float-zoned, Lopex*, and Czochralski crystals of various resistivities and dislocation densities. Three diffusion techniques have been investigated to introduce Li into the cell. The recovery of the cells, following high-energy-electron irradiation as affected by various manufacturing parameters, is also discussed. Cells for the initial shipments were made with the Li-suspension-paint-on technique, but the majority of the cells shipped on the contract were fabricated with evaporated Li. Equations for the vapor-phase diffusion of Li were developed and one group of vapor-diffused cells was shipped to NASA.

Investigations have been conducted into the various parameters affecting the Li diffusion, such as surface preparation, boron-doped layers, and Li coverage of the diffusion surface. Experiments of precipitation and out-diffusion of Li have also been carried out on Hall bars. The effect of high-temperature storage on Li-doped solar cells was also studied.

Integral quartz covers were successfully deposited on Li-doped cells and shipped to NASA for radiation testing.

A preliminary study was made to show the feasibility of using high-energy charged-particle irradiation to measure the oxygen concentration in Si at the 10^{14} cm^{-3} level.

---

* "Lopex" is a Texas Instruments Incorporated trade name for silicon with low oxygen concentration and low dislocation densities.

PRECEDING PAGE BLANK NOT FILMED.

SECTION II

TECHNICAL DISCUSSION

A. LITHIUM DIFFUSION IN SILICON

Several methods have been utilized for diffusing Li into Si for producing P-on-N solar cells. These are:

1) Li-in-mineral-oil suspension
2) Evaporated Li
3) Vapor diffusion
   a) Two-temperature
   b) Alloy or compound source

The relative merits of each of these are discussed in the following sections. Factors such as the presence or absence of an oxide film or a localized P^+ layer were studied, as were geometrical effects associated with the edges of a cell when using the paint-on method.

The boron-diffusion profile, as inferred from an incremental sheet-resistance measurement, is discussed, and precipitation data for lithium under several conditions are presented.

1. Lithium-in-Mineral-Oil Suspension

Most of the cells delivered during the first two months of the contract were diffused with Li using this method after the boron layer had already been diffused. The suspension was painted on the back of the cells, and the cell diffused in forming gas. To estimate a diffusion profile, the diffusions were performed in P-type material of several different boron concentrations and the P-N junction depth was monitored by sectioning and staining. Relationship of the junction depth x_j to the boron concentration at 400°C and 325°C is shown in Figure 1. This data, after any given diffusion, could be interpreted as the Li concentration profile if the diffusion constant and Li solubility were independent of boron concentration. However, both the solubility and the diffusion coefficient of Li are affected by boron concentration, especially at boron concentrations above the intrinsic carrier concentration n_i at the diffusion temperature (2 by 10^{16} cm^{-3} at 400°C). Hence the data should be considered as empirical. Note that x_j at 400°C at a given concentration does not follow the square root of time. The nature of the departure indicates that Li arriving at side B is diffusing out or reacting. The distribution is thus approaching a steady-state situation where the amount of Li entering at A is equal to that leaving at B. The high solubility of Li in heavily P-type material would make this even more probable if side B has a P-type solar-cell diffusion.

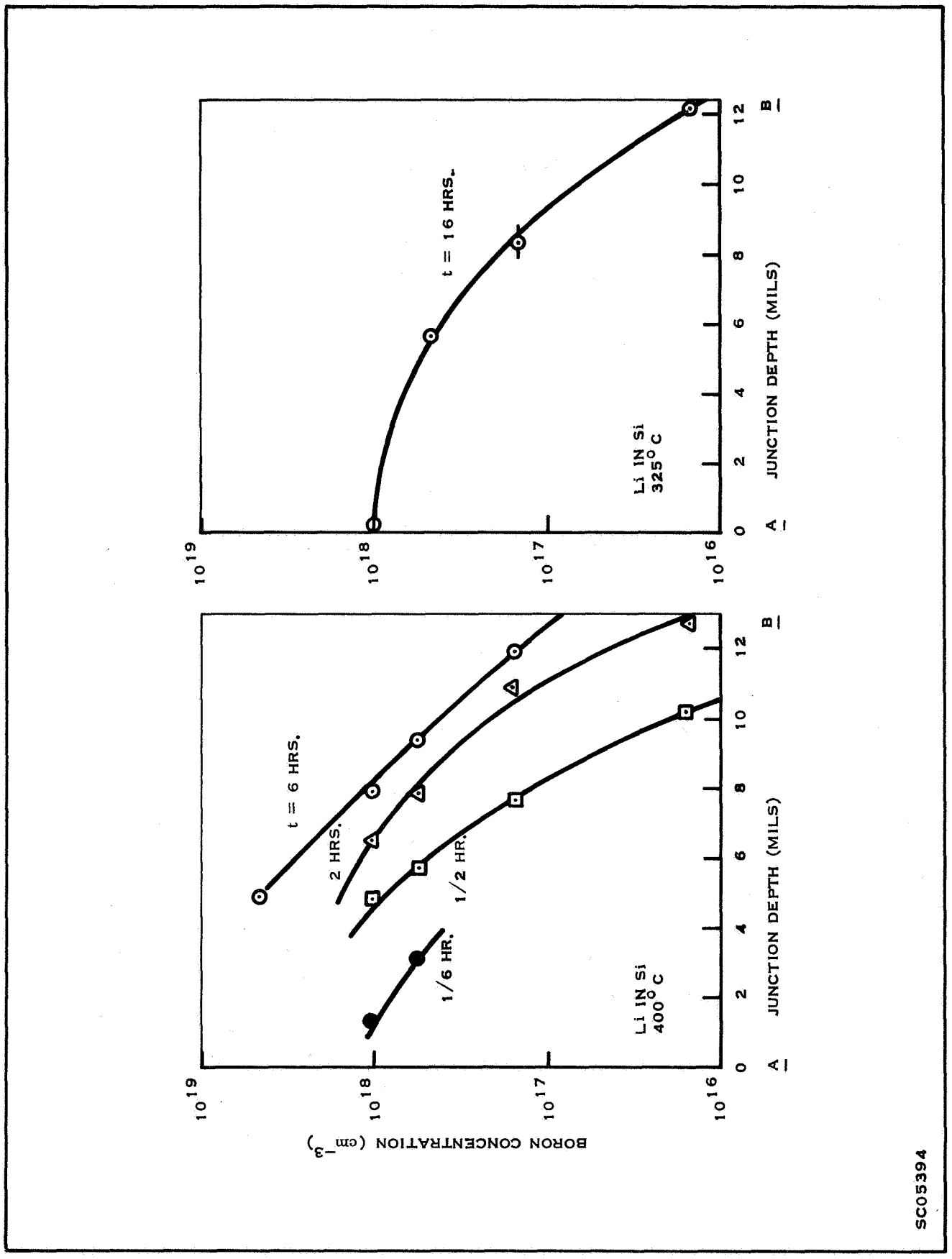

Figure 1. P-N Junction Depth in Si for Li Diffusion at 400°C and 325°C
(Li-in-Oil Suspension on Side A, Bare Side B, Forming-Gas Atmosphere)

a. Lateral Spreading

The form of the lateral spreading from a straight-edge source of Li, using the painted-on Li-in-oil suspension, is shown in Figure 2. Figure 3 is a 100X microphotograph of the junction developed in 1-Ω cm P-type material. The superposed photograph of the top surface shows the Li-alloyed region and P-N junction of the surface. The Li was diffused for 30 minutes at 400°C in forming gas. The data for various diffusion times are shown in Table I.

The above data were taken into account when cells were fabricated. To demonstrate the effect of uncoated edges, a series of runs of 2 hours at 400°C was designed with uncoated edges 0, 30, and 60 mils in width. These cells were sent to NASA-Goddard for evaluation of recovery properties. The results of this irradiation were consistent with expectations, the uncoated edges showing no recovery, although the effect was weaker than expected. For example, the cell areas represented by the uncoated edges in the 30- and 60-mil runs were about 20 percent and 40 percent respectively, yet the unrecovered damage after eight days represented decreases in cell efficiencies of only 11 percent and 20 percent of their initial values. Most of the difference in the former numbers can be explained by taking into account the lateral spreading of the diffusant.

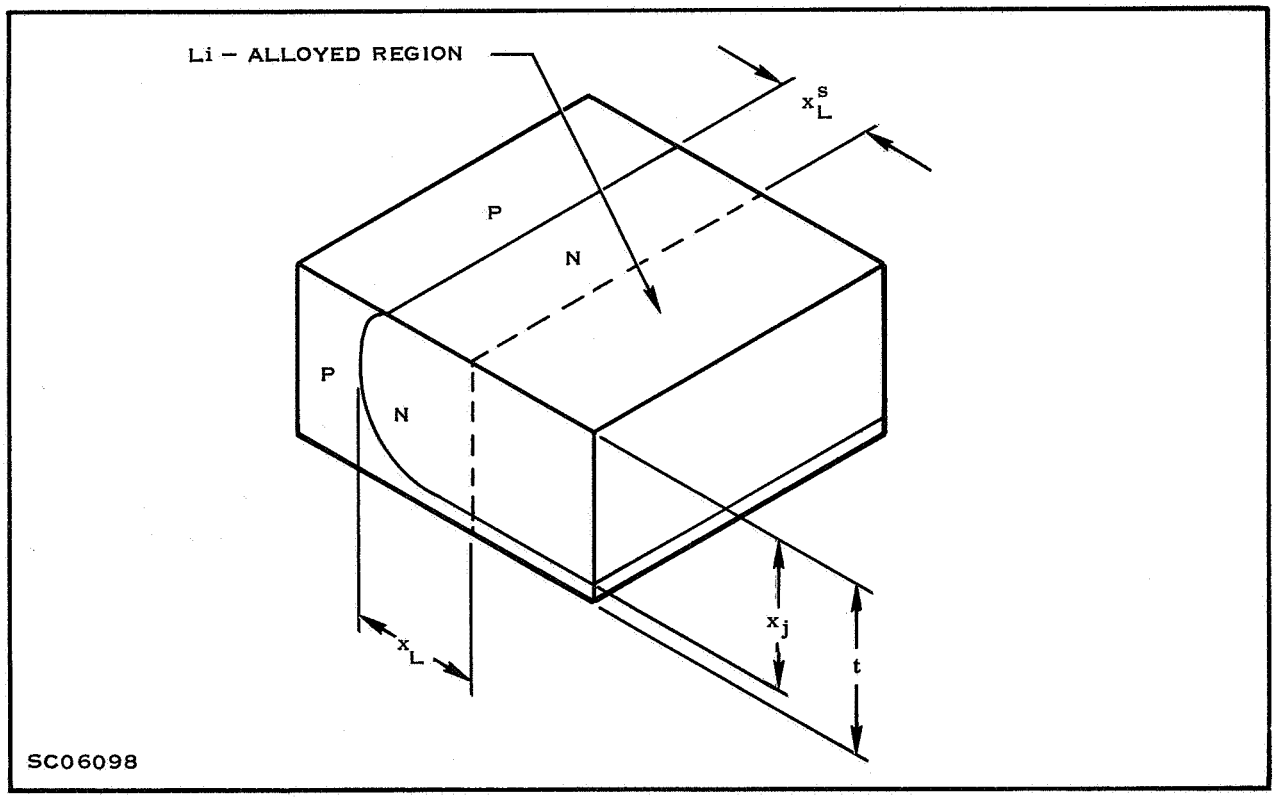

Figure 2. Lateral Spreading of Li in Si From an Edge Source

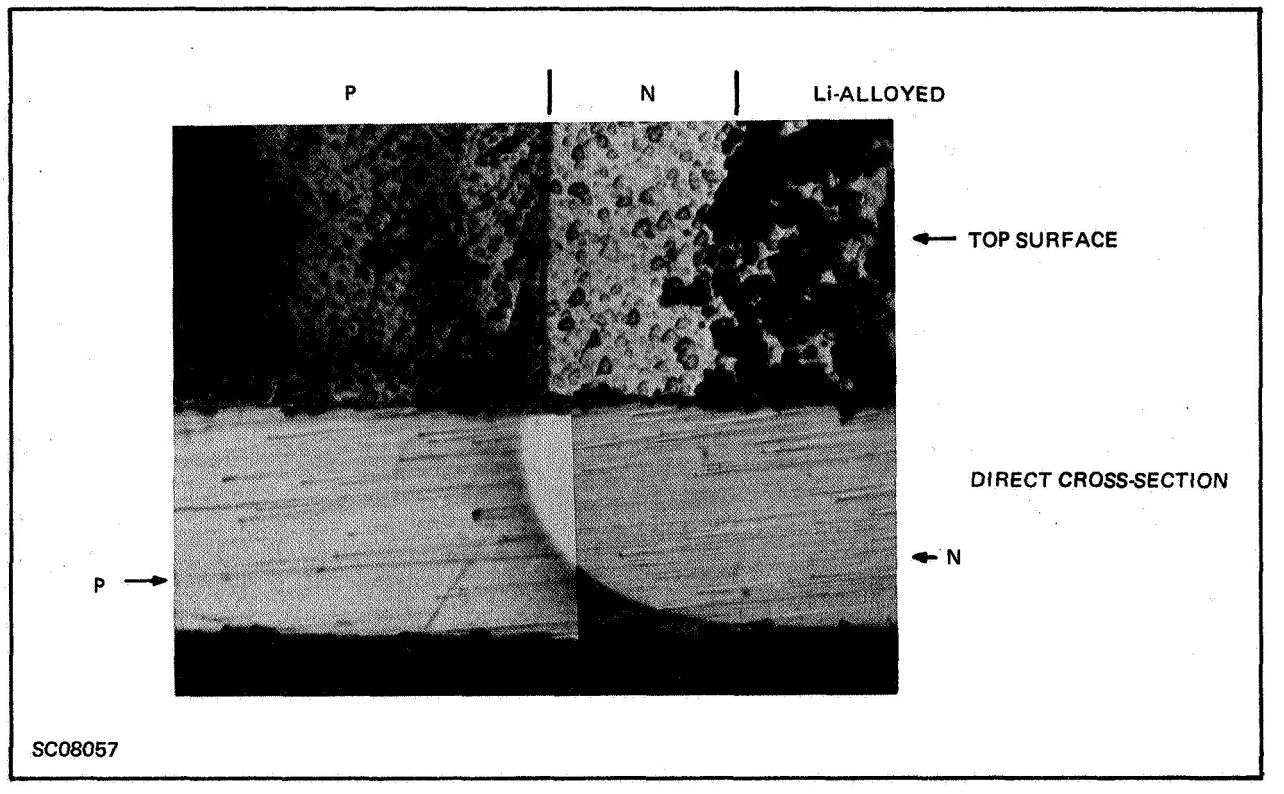

Figure 3. Microphotograph of Lateral Spreading of Lithium (30 Min at 400°C) (100X)

Table I. Values of Lateral Spreading and Other Penetration Distances

t (Hrs)	x^s_L (Mils)	x_L (Mils)	x_j (Mils)	σ (Mils)
0.5	8.0	9.5	11.8	12.2
1.0	10.0	11.5	>12.0	12.0
4.0	19.0	26.0	>18.0	18.0

By comparison, a cell coated on the back from edge to edge recovered to 93 percent of its initial value. All these figures apply to an integrated flux of 1 by $10^{14}/cm^2$ of 1-MeV electrons in a period of 20 minutes. A similar integrated flux of 0.5-MeV electrons recovered almost completely (to 99 percent of its initial value) for a cell coated edge to edge. We will discuss the recovery of the standard cell in Section G.

b. Surface Preparation

Sand-blasted and etched surfaces give identical junction depths, with the alloying slightly more uniform on the sand-blasted surfaces. However, non-uniform alloying is not serious as long as the unalloyed regions are much smaller than the penetration depth.

c. Effect of Boron-Diffused Layer

At 400°C the lithium solubility can be enhanced significantly by boron.[2] However, at a concentration of boron above 4 by $10^{18}cm^{-3}$ a crystal remains P-type after Li diffusion, although with a significant increase in resistivity. This increase in resistivity is quite pronounced in the boron-diffused layer during vapor diffusion of lithium (see Section II.A.3.b.(3)).

The effect of a boron-diffused layer on the front surface, during lithium diffusion from the back, was also studied. The lithium diffusion was not measurably affected as compared to similar runs with no boron-diffused layer present. Similarly, a thin boron-diffused layer on the back where the lithium suspension was applied was easily penetrated by the lithium. Both effects were studied by monitoring the junction depth in P-type material in slices in which the boron-diffused layer had been removed on one-half of the slice. In view of the large built-in electric field and the sharply enhanced Li solubility in the boron-diffused layer, this is a surprising result. In the case of a boron layer on the side where the Li is applied, it evidently stems from the extreme shallowness of the layer, which allows dissolution of the Si to a depth greater than that of the boron-diffused layer.

2. **Evaporated Lithium**

The solar cells delivered during the major portion of the contract were fabricated by diffusing from a thin layer of Li on the back of the slice. This layer was vacuum evaporated through a mask which left 20 mils of the edge uncoated. The results obtained regarding junction depth were very similar to those when using the painted-on suspension, but there was much less surface damage on the back surface after diffusion. Cell reproducibility was also improved compared to that when using the painted-on method.

3. **Vapor Diffusion of Lithium**

A vapor-diffusion process for Li was also studied. This should result in better control of the Li concentration than is possible using either the evaporated-layer or painted-on-suspension techniques. It should also eliminate any edge effects of the type discussed earlier.

a. Theoretical Discussion

The amount of Li entering the crystal from the vapor is dependent on the chemical "activity" of the Li in the vapor phase. The activity is proportional to the Li partial pressure. Methods of reducing the activity are: (1) Li-metal alloy such as Li:Sn[2]; (2) Li compounds such as Li_2O or LiBr[3], and (3) a two-temperature method in which the Li is kept at the cold end of a sealed ampoule. These methods are discussed under b, Experimental Results. General equations for the vapor diffusion of lithium are given herewith.

The Li dissolution in the silicon can be represented by

$$Li_{gas} \rightleftharpoons Li_I^{\circ} \qquad (1)$$

where Li_I is un-ionized when it first enters the Si lattice. The subscript I is a reminder that Li enters the crystal as an interstitial impurity. The mass-action expression for Equation (1) is

$$(Li^\circ) = K_1 P_{Li} \tag{2}$$

where P_{Li} is the Li pressure in the ampoule. The Li_I° subsequently ionizes by the reaction

$$Li_I^\circ \rightleftharpoons Li_I^+ + e^- \tag{3}$$

which can be represented by

$$\frac{(Li_I^+)\, n}{(Li_I^\circ)} = K_D \tag{4}$$

where n is the electron concentration and

$$K_D = N_C \exp \left[(E_D - E_C)/kT\right]$$

with N_C the density of states in the conduction band at the diffusion temperature. E_C and E_D are the conduction band and Li donor ionization energies respectively. A conservation condition gives

$$(Li_I^+) + (Li_I^\circ) = (Li_I) \tag{5}$$

where (Li_I) is the total Li concentration in the silicon. The charge neutrality condition gives:

$$n + (A^-) = p + (Li_I^+) + (D^+) \tag{6}$$

where p is the hole concentration and (A^-) and (D^+) are the ionized acceptor and donor concentrations already present in the crystal. These will be assumed negligible in the present calculation. The hole concentration p will be negligible at high Li concentrations if Li is the dominant impurity. However, the hole concentration cannot be ignored at low Li concentrations when $(Li_I) \leqslant n_i$, the latter symbol denoting the intrinsic electron concentration at the diffusion temperature. Finally, using Equations (2) and (6) to solve Equation (5) for the Li solid solubility in terms of the vapor pressure of Li yields

$$(Li_I) = n - p + (Li_I^\circ) = n - p + K_1 P_{Li} \tag{7}$$

This equation is easily solved in the following cases:

Extrinsic Case. Under extrinsic conditions, namely, $Li_I^+ >> n_i$, p is negligible and also $n = Li_I^+$. Under such conditions Equation (7) becomes

$$(Li_I) = \left[K_D K_1 P_{Li}\right]^{1/2} + K_1 P_{Li} \tag{8}$$

where the quadratic term and linear term represent (Li_I^+) and (Li_I°) respectively. Since extrinsic conditions exist at the solid solubility limit of Li, it is possible to evaluate K_1 at any temperature. This follows from a knowledge of the solid solubility of Li in silicon[5] along with the vapor pressure of Li at the diffusion temperature.

Intrinsic Case. At very low Li pressures the Li concentration in the silicon becomes less than the intrinsic electron concentration. Furthermore, the postively charged Li is the major portion of the Li, so the total Li concentration is given by

$$(Li_I) = (Li_I^+) = \frac{K_D K_1 P_{Li}}{n_i} \qquad (9)$$

b. Experimental Results

(1). Two-Temperature Technique. The experimental results using the two-temperature technique do not fit the predictions of the above, the amount of Li introduced into the silicon being 10 to 100 times too low. The cause for this is evidently the reduction of chemical activity (or vapor pressure) of the Li in the vapor by reaction with the quartz ampoule. Attempts to overcome this difficulty by saturating the quartz walls with Li were not successful. Passivating the walls of the ampoule with graphite was also unsuccessful in this regard.

(2). Alloy Source. Diffusion from an alloy source of Sn and Li (0.80 wt % Li) at 400°C for 20 hours in an evacuated ampoule resulted in N-type silicon of resistivity 0.4 to 0.6 Ω-cm. This is close to the results obtained by Reiss and Fuller[2] using a 0.63 wt % Li:Sn alloy. However, they immersed their samples in the alloy, which in our application would damage the solar-cell surfaces badly. Their results at several temperatures are shown plotted in Figure 4 for the 0.63 percent alloy along with our results at 400°C. The agreement is not perfect, but was close enough to justify fabricating cells. A small lot was processed using this method and shipped to NASA-Goddard for electron irradiation and evaluation. Cell recovery was much less pronounced than with cells doped from the back surface. This is probably due simply to a smaller Li concentration in the vicinity of the junction.

(3). Compensation of P-Type Layer. The sheet resistance of the boron-diffused layer increased significantly during the diffusion treatment from an alloy source. For example, the value typically increased from 25 ohms/square to 50 to 70 ohms/square. (Less than 10 percent change in sheet resistance was observed in cells using the evaporated-Li procedure.) This increased sheet resistance is not surprising in view of the Li solubility enhancement in heavily doped P-type material, as demonstrated in Figure 4. The expected compensation level of the boron acceptors by the Li donors from this graph is about 60 percent in the 400°C range; i.e., 40 percent of the boron atoms should remain electrically active. Thus the average resistivity should increase about 2.5 times, which is very close to what was observed. At lower temperatures even more compensation is predicted, so the cooling rate may be a significant factor in the final sheet-resistance value. Rearrangement of the Li in the vicinity of the P-N junction after cooling should be expected for a considerable period. This is accentuated by the enhanced Li solubility at lower temperature observed in boron-doped Si (Figure 4).

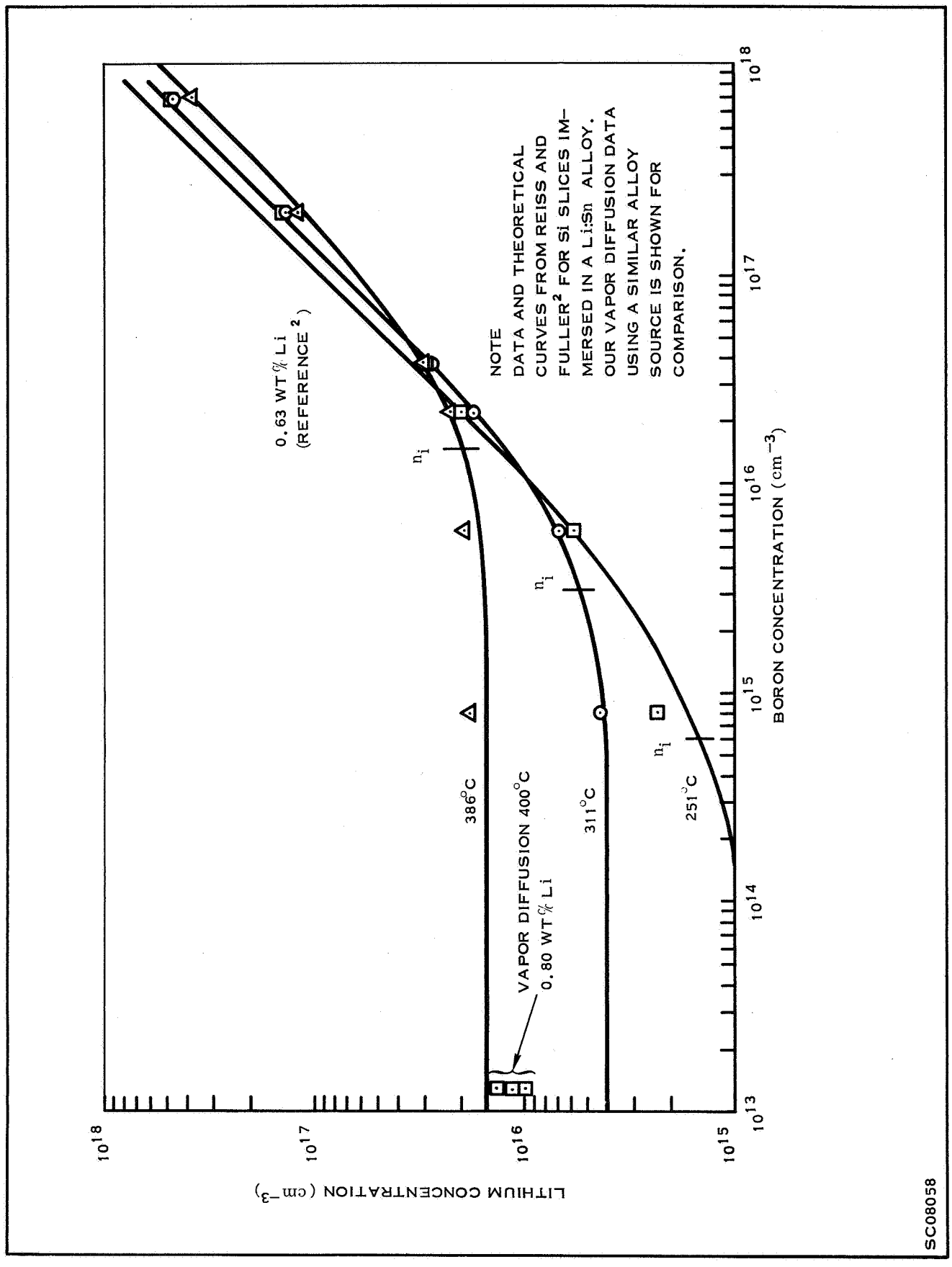

Figure 4. Lithium Saturation Results

(4). Oxide-Layer Effect. The effect of a 600-Å thermally grown oxide layer over part of a Si slice was also monitored by observing the junction penetration into P-type material during a vapor-diffusion experiment. The junction depth was identical to that in the uncoated region, suggesting that a SiO_2 layer of this thickness is not a barrier to Li penetration.

4. Other Diffusion Methods

A great deal of effort was expended to find a diffusion process that could be applied in a controlled fashion over a wide range of Li concentration at any temperature in the 300 to 600°C temperature range. One of the main requirements we placed on such a process was that the Si surface not be damaged, since the primary application was the Li diffusion of solar cells with a thin boron-diffused layer already applied.

As mentioned earlier with regard to the two-temperature method, the major problem encountered was the continuing reaction of Li with the quartz ampoule, which served to reduce the Li vapor pressure in the container. The extreme reactivity of Li was also evident in several unsuccessful attempts to pass a Li containing inert gas over the Si slices in an open-tube furnace. Trace concentrations of oxygen, nitrogen, and water vapor were probably responsible for the reaction of Li in these cases.

One such method taken from the recent literature[6] was partially successful in this regard, in that a Li concentration near the solid solubility could be attained at a given temperature without surface damage. However, we were not successful in controlling the concentration below this value. The method involves the continuous evaporation of Li upstream from the Si samples and carrying the Li in a steady argon flow past the Si samples. The success of the system apparently is due to a very thin evaporated layer being present on the samples. When the flow is too low to provide such a film, the Li chemical activity or vapor pressure at the Si interface evidently decreases drastically.

A technique that seems promising is the "sandwich approach," in which three Si slices are stacked together. The two outer slices have one face each which contains evaporated Sn:Li of a given concentration. The inner slice begins to be permeated with Li when the Li has diffused through the two outer slices. This technique results in no surface damage, but is still somewhat variable due to the reaction of the Li in the alloy with the quartz ampoule. This causes the Li concentration in the alloy to decrease during the diffusion run. This decrease can be obviated by operating in one of the two-phase regions of the Sn:Li phase diagram, since the chemical activity must be constant across one of these regions. Thus by operating on the Li-rich side of one of these two phase regions, some loss of Li can be tolerated and still not affect the Li surface concentration in the Si. It is expected that this concept will be explored in detail in the next contract with NASA (through the Jet Propulsion Laboratory).

B. CARRIER LIFETIME IN Li-DOPED SILICON

Several samples of high-resistivity Si were diffused throughout with Li, using the Sn:Li alloy as a vapor-diffusion source. The Li concentration was varied from 10^{15} cm^{-3} to 2 by 10^{16} cm^{-3} by varying the weight percent of Li from 0.1 to 1.5 percent. The diffusion runs were carried out at 400°C for 18 to 72 hours. Starting material ranged from 20 to 40 Ω cm N-type (phosphorus doped).

The lifetime (τ) measurements were made by J. B. Horak[7] using the surface photovoltage (SPV) method.[8] Note in Figure 5 that there is no apparent difference in τ for Li-doped Si as compared to Sb- or P-doped Si. However, Lopex material generally has longer τ's than float-zoned or pulled crystals regardless of doping.

C. BORON PROFILE DETERMINATION

The boron diffusion profile has been determined using incremental sheet resistance measurements along with a boiling water-HF sequence for sectioning. The junction depth was found to be 5200 ± 400Å in the cell measured (20 Ω-cm bulk). The maximum electrically active boron concentration was 2 to 3 × 10^{20} cm^{-3} at a depth of 1000Å (see Figure 6). Note also the pronounced "slumping" in the 500-Å zone near the surface. This is probably due to out-diffusion on the cooling cycle.

The cells were sectioned using boiling-water oxidation (1 to 2 minutes) followed by a HF rinse.[9] The removal rate varied between 13 Å/step and 30 Å/step. There was little difference between the 1-minute and 2-minute boiling steps. Contaminating layers slowed the oxidation in certain regions so the sectioning was not as uniform as expected. There was no evidence that the oxidation rate slowed in the vicinity of the junction, as predicted by Beck,[9] but the contaminating layers may have masked such an effect.

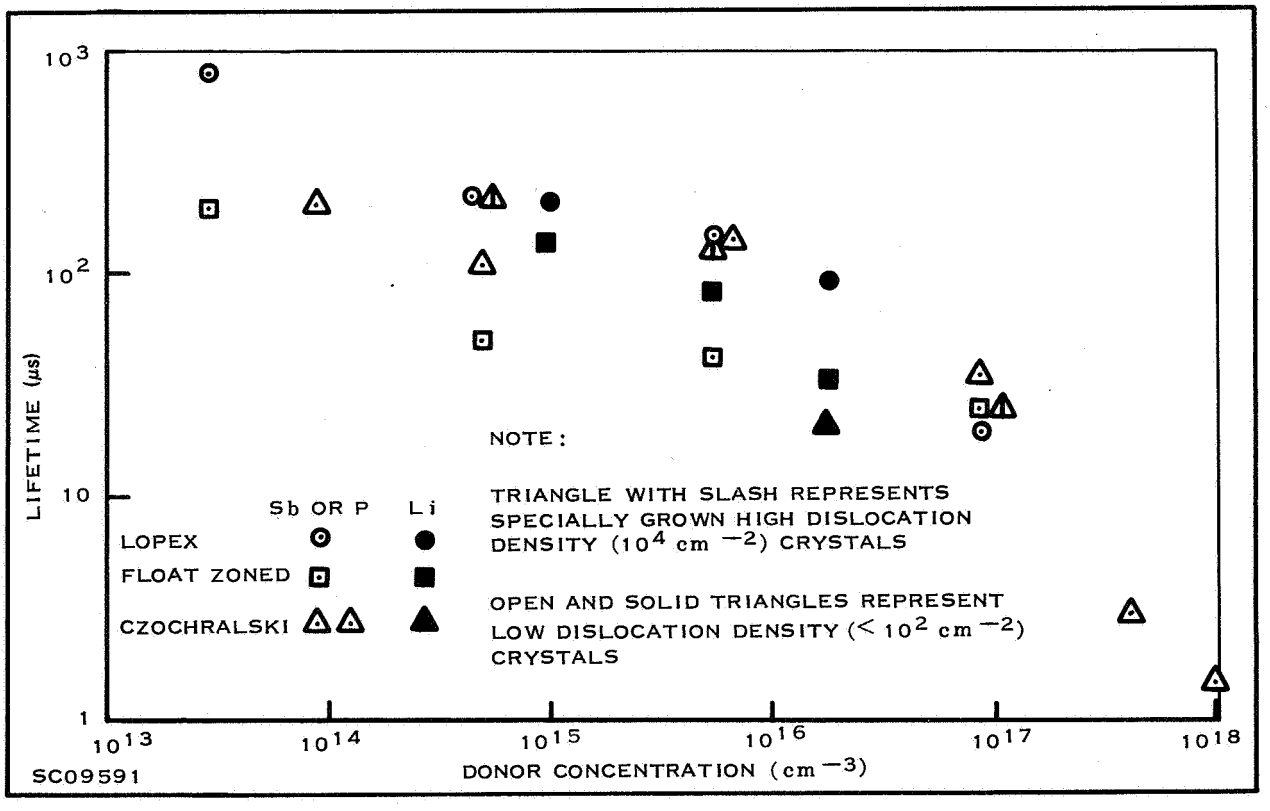

Figure 5. Minority Carrier Lifetime of N-Type Silicon Crystals versus Concentration of Li, Sb, and P

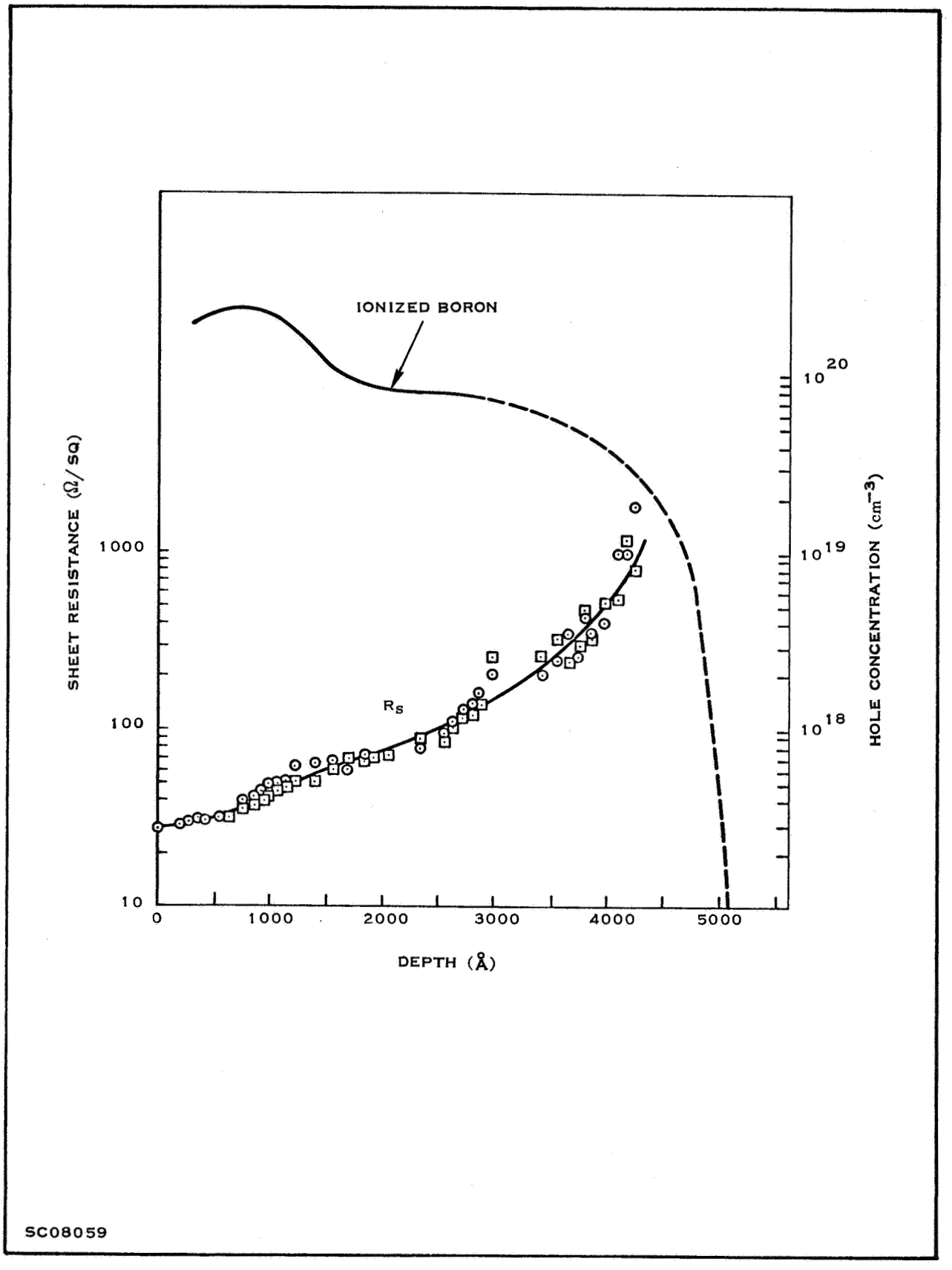

Figure 6. Boron Diffusion Profile Prior to Lithium Diffusion

D. PRECIPITATION AND/OR OUT-DIFFUSION OF LITHIUM

Samples of Lopex, and quartz-crucible-pulled, 20-Ω-cm, N-type Si were diffused with Li using Li-in-oil-emulsion on both sides for 48 hours at 325°C in forming gas, and the slices were cut into Hall bars of 14 mils thickness. To accentuate the oxygen donor reaction[10] in the crucible material, the slices were heat treated prior to Li diffusion at 450°C for 16 hours in forming gas. The average resistivity following the Li cycle was 0.06 Ω-cm, which corresponds to a Li concentration of 2×10^{17} cm^{-3}. The samples were then heat treated at 200°C for 30 hours, while electrical measurements were taken at 27°C every hour for the first 6 hours and about every 4 hours thereafter. The average resistivity of both the Lopex and pulled samples approximately doubled during the 30 hours' treatment. If the same process of precipitation and/or out-diffusion were operative at room temperature, and if the rate were dependent only on the diffusion rate of Li, a similar amount of reaction at 27°C would require about 70 years. This cannot be assumed a priori to be accurate, however, since the effectiveness of the precipitation centers may be a function of temperature. The degree of super-saturation is also important in this regard. This is very evident in the Li precipitation results of Pell[11], whose results predict a precipitation time of only one minute to achieve a factor of 2 increase in resistivity at 200°C in Si doped to 10^{19} cm^{-3}.

For a more accurate estimate of the effect of Li precipitation and/or out-diffusion, annealing runs on the actual solar cells at several temperatures have been made. These tests will be discussed in Section F.2.c.

E. ISOCHRONAL ANNEALING

Several samples of Li-diffused Si in the shape of Hall bars were heated for 20 minutes at 50°C in a forming-gas atmosphere, after which the apparent resistivity at room temperature was monitored. This was repeated at 100°C, 150°C, etc. up to 1200°C. Electrical contacts were applied at room temperature after each heat treatment, using an amalgam of Hg, In, and Tl. This was then cleaned off in HCl before the next heat treatment. The samples were lightly sandblasted before the 450°C treatment to remove any surface conduction paths. The results are shown in Figure 7 for two different resistivities in Lopex and float-zoned starting material. The lower-resistivity material was prepared using the paint-on-Li-oil technique mentioned above (48 hours at 325°C). The higher ρ material was prepared by a Sn:Li vapor diffusion process at 400°C. All the samples were 15 to 20 ohm-cm N-type (phosphorus) before Li diffusion except sample 5C, which was 0.9 ohm-cm P-type (boron) before Li diffusion.

From these data it appears that the Li begins to precipitate or out-diffuse at an appreciable rate at 300°C and the precipitation or out-diffusion is complete under these conditions at 550°C. This is consistent with a simple out-diffusion model which predicts that the concentration at the center of a 14-mil slab should drop to 10 percent of initial value in 25 minutes at 550°C.

The decrease in ρ at 250°C in the two 0.5-ohm-cm samples is quite surprising. It suggests that a defect complex is dissociating in this temperature range and contributing more donors (and hence electrons) to the system. These anneal in the same temperature range. An example of such a process would be the dissociation of a Li_4O complex into isolated Li interstitials, as Pell proposed in

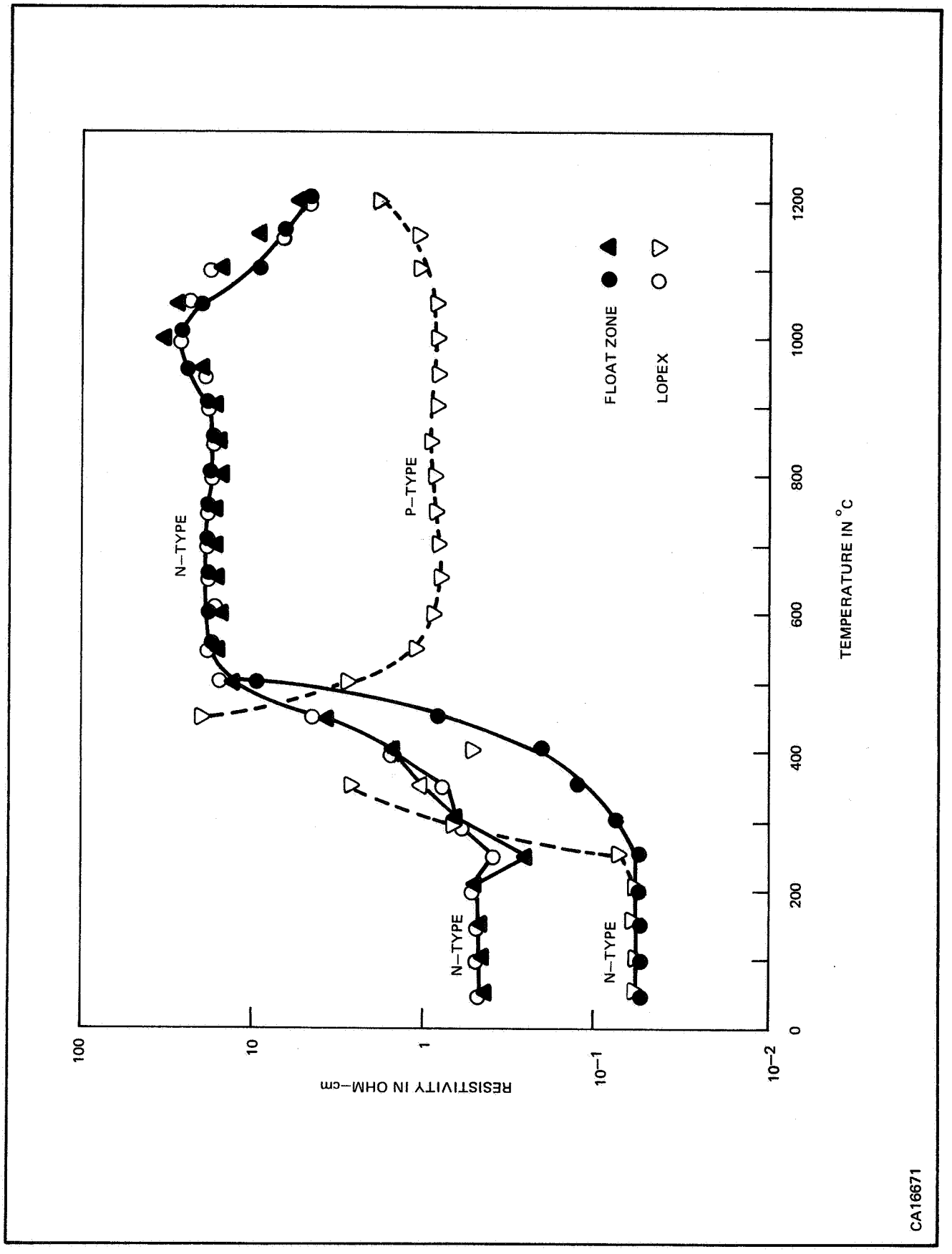

Figure 7. Room-Temperature Resistivity After Isochronal Annealing

explaining some of his Li-precipitation data.[11] The changes above 900°C are due to furnace contaminents. The discontinuity in ρ of the originally P-type crystal is due to the transition from N-type to P-type after heating in the 400°C range.

F. SOLAR-CELL FABRICATION

1. Basic Fabrication Process

The basic process in the fabrication of lithium-diffused solar cells is outlined in the simplified process flow diagram of Figure 8.

The processing steps, from the manufacture of the silicon through the chemical polishing of the blanks, were performed by the Chemical and Materials Division of Texas Instruments. The rest of the processing steps were performed by the Solar Cell Development Group of the General Products Department. The lithium-vapor-diffusion process development was performed by the Semiconductor Research and Development Laboratories (SRDL) of Texas Instruments.

Most of the cells fabricated for the contract were 1 cm X 2 cm, 3 grid, Ti-Ag solderless, 13 mils nominal thickness. One group of cells was solder coated (those discussed in F.2.e.).

2. Process Variables

The primary processing variables investigated have been the crystal type (Lopex, float-zoned, and Czochralski); initial base resistivity; dislocation density; oxygen content; and lithium-diffusion parameters. Table II shows the silicon material variables investigated on the contract as originally planned. The Li-diffused cells which showed the highest initial conversion efficiencies were fabricated from 10-to-100 Ω-cm Lopex and float-zoned material.

a. Sintering

The sintering operation has been evaluated on a number of runs. Table III shows the electrical characteristics of sintered and unsintered cells of various crystal types. All the cells in the experiment were 15-to-25 Ω-cm base resistivity. The lithium evaporation and diffusion were performed as two operations; that is, all the cells in the table listed as 450°C diffusion were processed in one Li-evaporation-and-diffusion run. The diffusion was performed in a furnace immediately after Li evaporation.

Two cells from each group were subjected to the contact pull test. There were no contact failures on any group. However, the silicon broke on some of the cells at pull strengths in the 100-to-500-gram range on both the sintered and unsintered groups. The 12 unsintered and the 12 sintered cells averaged 966 grams and 2058 grams, respectively, on pull test.

The recovery of the short-circuit current of these cells after a $10^{14}/cm^2$ dose of 1-MeV electrons is shown in the last column of Table III after various times at room temperature. The Lopex cells generally had the highest efficiency and recovered more quickly than the float-zoned

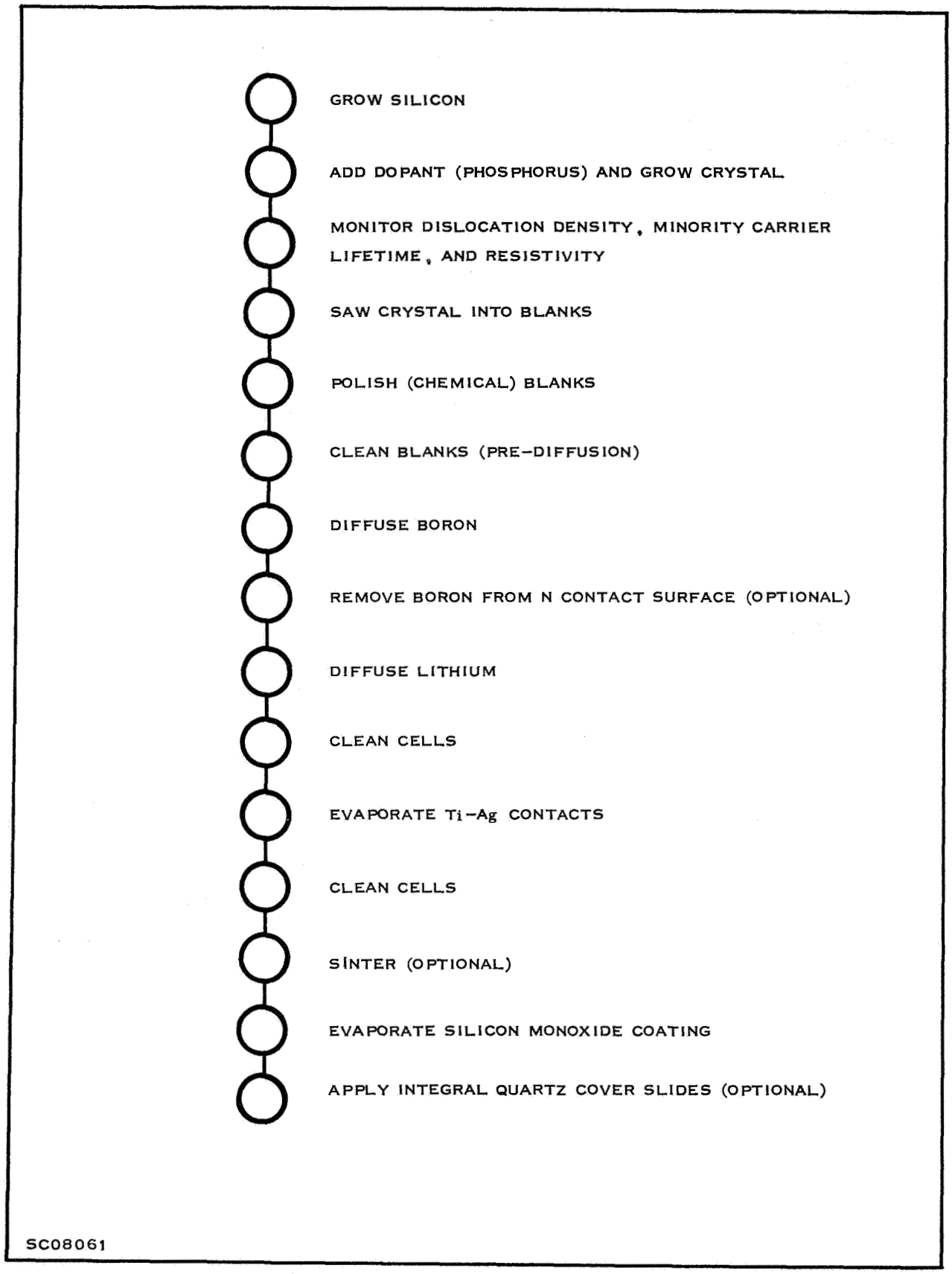

Figure 8. Lithium-Diffused Solar Cell Process Flow Diagram

Table II. Material Matrix of Lithium-Diffused Solar Cells

Nominal Resistivity (Ω-cm)	N-Dope	Oxygen Content (Atoms/cc)	Dislocation Density
0.1	Phos	$<10^{17}$	High (10^4 to 10^5)
1	Phos	$<10^{17}$	(Float-Zone)
10	Phos	$<10^{17}$	(Float-Zone)
20	Phos	$<10^{17}$	(Float-Zone)
100	Phos	$<10^{17}$	(Float-Zone)
20	Phos	$<10^{17}$	Very High (10^5 to 10^6) (Float-Zone)
0.1	Phos	$<10^{17}$	Very Low
1	Phos	$<10^{17}$	(Lopex)
10	Phos	$<10^{17}$	(Lopex)
20	Phos	$<10^{17}$	(Lopex)
100	Phos	$<10^{17}$	(Lopex)
20	Phos	High (10^{18})	10^3
20	Phos	High (10^{18})	10^4 to 10^5 (Pulled)

cells. However, the Lopex cells degraded again (redegraded) at long times. We now believe that the faster recovery and redegradation of these Lopex cells are due mainly to higher lithium concentration in the junction region. This was probably caused by small differences in cell thicknesses between the Lopex and float-zoned cells in the above runs. This effect will be discussed in more detail in Section G.

The sintering was done at about 600°C for 3 minutes. This is equivalent to about one additional hour of diffusion at 400°C with no diffusion source. There is little difference in the electrical properties or the radiation recovery of the cells, but the pull-test data mentioned above suggest that sintering the cells is probably helpful.

b. Dislocation Density

Cells were processed to study the effect of dislocation density on cell and radiation recovery characteristics. Material from two 15-to-25-ohm-cm float-zone crystals was used for the test. Samples were cut from each crystal, and the dislocation density was determined to be 35,000 per cm^2 for one and 74,000 per cm^2 for the other crystal.

Table III. Electrical Characteristics of Lithium-Diffused Silicon Solar Cells

Group	Conditions	I_{SC}‡ (mA)	V_{OC}‡ (mV)	Eff. ‡ (% AM1)	Qty. Shipped	Fraction Recovered 3,5,120 hrs.††
1	Pulled, 450°C, 30 min., sintered	51–55	565–588	10.0–11.3	4	
2	Pulled, 450°C, 30 min., not sintered	50–53	453–568	<10%	0	
3	Pulled, 400°C, 2 hr., sintered	53–55	575–602	10.4–12.3	7	
4	Pulled, 400°C, 2 hr., not sintered	54–55	585–600	11.3–12.2	5	
5	Lopex, 450°C, 30 min., sintered	54–57	590–603	11.9–13.0	8	.85, .88, .85^{r}
6	Lopex, 450°C, 30 min., not sintered	54–56	591–603	11.9–13.0	6	.89, .90, .87^{r}
7	Lopex, 400°C, 2 hr., sintered	57–58	593–604	12.7–13.6	8	.88, .90, .85^{r}
8	Lopex, 400°C, 2 hr., not sintered	55–57	589–605	12.0–12.9	6	.89, .90, .87^{r}
9	F. Z., 450°C, 30 min., sintered	51–57	575–590	10.5–12.4	7	.86, .88, .89
10	F. Z., 450°C, 30 min., not sintered	52–56	573–594	11.3–12.4	6	.81, .83, .88
11	F. Z., 400°C, 2 hr., sintered	52–56	573–598	11.0–12.5	8	.86, .88, .92
12	F. Z., 400°C, 2 hr., not sintered	51–53	580–595	11.1–11.8	5	.84, .87, .92

‡ 100 mW/cm^2 tungsten source

†† Nominal times

r Redegradation

Silicon blanks were fabricated from each crystal, identified, and processed in the same boron diffusion run. Cells were processed as one production lot to minimize process variations on each group. Table IV gives the results of this test. Cells No. 226 through 270 and 271 through 310 were processed in a single Li evaporation-diffusion run of 400°C for 2 hours and 450°C for 30 minutes respectively.

The dislocation densities specified in the table are the values for the samples cut from the bottom of the crystals, Dislocation densities were measured on solar-cell blanks taken from each crystal before and after boron diffusion. There was no detectable increase in dislocation density due to the boron diffusion cycle, at least at a depth of 4 microns below the surface.

c. Cell Heat Treatment

In order to predict more accurately the long-term behavior we have heat-treated solar cells at 250°C (Figure 9) and 150°C. The efficiency of these cells dropped to about 90 percent of their initial values after 20 hours and 800 hours respectively. If out-diffusion of Li is the primary cause of

Table IV. Cell Characterization

Cell No.	Dislocation Density ($e.p./cm^2$)	Li Diffusion	Average I_{sc} (mA)	Avg. VOC (mV)	Avg. 0.430 V (mA)	Qty. Shipped
226 through 247	3.5×10^4	400°C-2 hrs	50.9	581	46.3	20
248 through 270	7.5×10^4	400°C-2 hrs	50.0	589	47.8	22
271 through 287	3.5×10^4	450°C-30 min	49.4	587	46.0	13
288 through 310	7.5×10^4	450°C-30 min	47.7	589	44.8	17

degradation of the Li-doped solar cell, a significant change should be evident when the out-diffused zone is the same order as the minority carrier diffusion length; namely, about 100 microns. Diffusion coefficients of Li and Si at these two temperatures are 10^{-9} and 4 by 10^{-11} cm^2sec^{-1}. Using a simple out-diffusion model, concentration of a previously uniformly doped sample (at C_o) would drop to 1/2 of its pre-diffused concentration at a depth specified by the expression $C/C_o = 1/2 = \text{erf } x/2\sqrt{Dt}$. This is satisfied when $t = x^2/D$, since erf 1/2 = 1/2. This assumes that the surface is an infinite sink for Li and that the Li concentration drops to zero at the surface. Assuming the active zone of the cell to be 100 microns, the calculated times at 250°C and 150°C are 29 and 700 hours respectively. These values are in adequate agreement with the values measured on actual solar cells. An important point is that precipitation in the bulk need not be invoked to explain the effect of the heat treatment of these cells. This is also consistent with the isothermal and isochronal annealing data of Sections D and E. However, radiation damage centers may initiate precipitation in the cells and vitiate the above conclusion, especially at high damage rates where clusters are more likely to form.

Extrapolation of the above results to lower temperatures suggests that lithium-diffused cells should degrade by a similar amount in periods of 30 and 200 years at 50°C and 27°C respectively.[4] However, one must qualify these estimates since they were not undertaken in a sunlit-high-vacuum-radiation environment. One test under roughly simulated space conditions at 100°C was performed. This is shown in Figure 10.

d. Integral Protective Shield

Integral coverslides of nominal 1-mil thickness were applied to the CeO_2-coated cells and one-half of each group of the SiO-coated cells. The 7940-fused-silica layer was deposited by RF sputtering at a deposition rate of approximately 1500 Å/min and a substrate temperature of less than 70°C. Table V shows the electrical parameters of the various groups under 100 mW/cm^2, sunlight-equivalent tungsten light, and cell temperature of 28 ± 1°C. Twenty N/P cells with CeO_2 coating and nominal 1-mil integral coatings were also tested and shipped against the contract.

The electrical properties of one of the integral coated-over-SiO-lithium cells, both before and after the coating, are shown in Figure 11. It is interesting to note that the float-zoned cells with a nominal 1-mil-thickness integral coating over the CeO_2 anti-reflective coating have higher

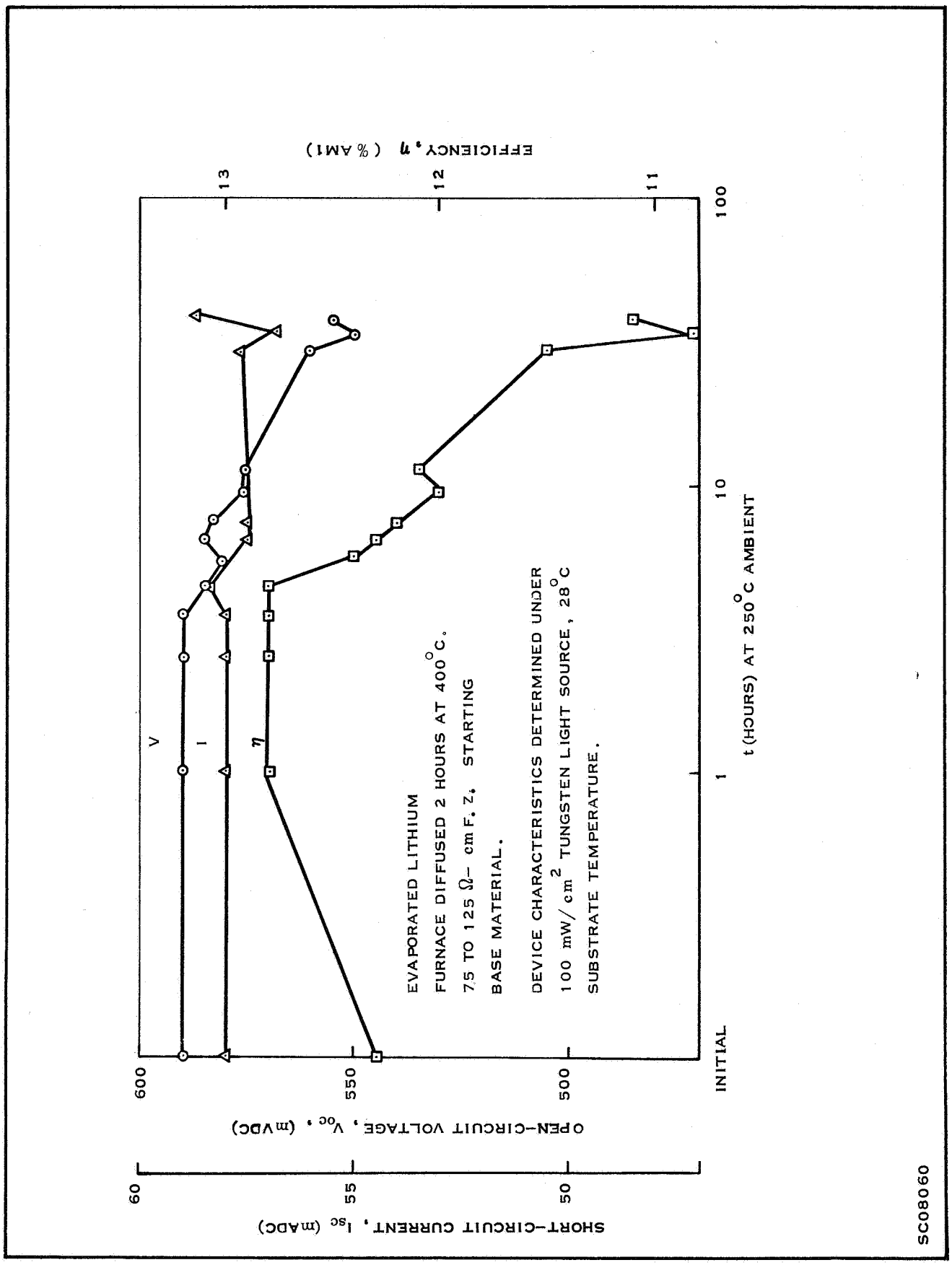

Figure 9. Device Characteristics Following 250°C Heat Treatment

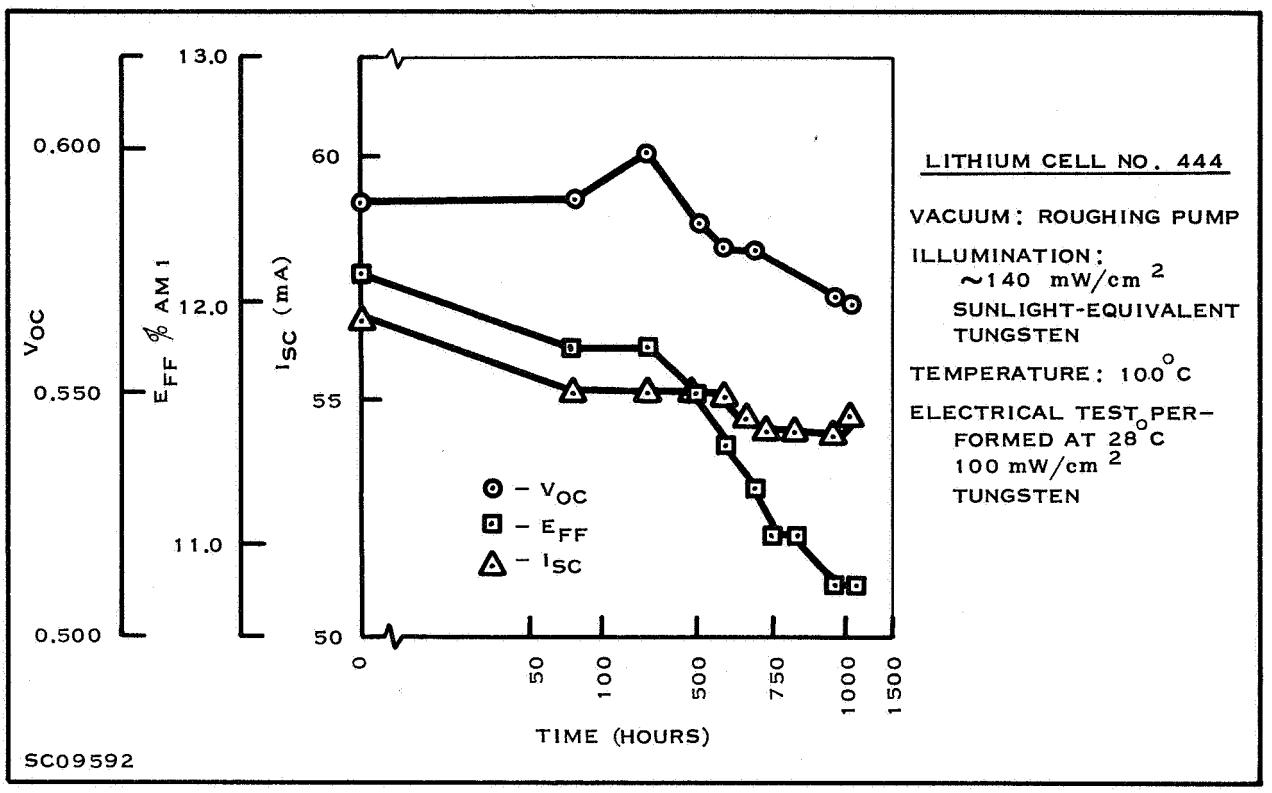

Figure 10. Environmental Test on Lithium-Diffused Cell

conversion efficiency than float-zoned cells with silicon monoxide coating only. The CeO_2 plus integral quartz coating is a better refractive index match between silicon and air than is silicon monoxide, resulting in lower reflection loss of light and, consequently, higher-efficiency cells.

e. Effect of Li Diffusion Time

Cells were processed to study the effect of the lithium diffusion cycle on conversion efficiency and radiation resistance in float-zoned (fz, Lopex (lx), and Czochralski (Cz) material of 15-to-25-Ω-cm resistivity. Table VI shows the average electrical parameters of each group at various diffusion times at 400°C. The data were taken under 100 mW/cm^2 tungsten at a cell temperature of 28 ± 2°C. The data are presented only to show the difference between the groups and should not be interpreted as absolute readings, since the light source was calibrated with N/P standards. Cell characteristics are relatively independent of diffusion time over the range covered, so a decision regarding optimum time should depend on radiation-damage annealing or other properties.

The lithium was introduced into the cells by evaporation through a 0.020-inch picture-frame contact mask and subsequently diffused at the specified times. The material listed under each diffusion time was processed in the same lithium evaporation and diffusion cycle.

Table V. Electrical Parameters

Cell No.	Description	Si:SiO_2 Intermediate Anti-reflective Coating	Average I_{sc}(mA) Pre-Integral	Average I_{sc}(mA) Post-Integral	Average V_{oc}(mV) Pre-Integral	Average V_{oc}(mV) Post-Integral	Average I at 430 mV(mA) Pre-Integral	Average I at 430 mV(mA) Post-Integral	Quantity Shipped
1114→1143	Czochralski Crystal >35 Ω/cm	CeO_2	55.8	56.6	581	577	50.4	49.9	30
1144→1181	Float-Zoned Crystal >195 Ω/cm	CeO_2	56.7	56.8	580	576	51.3	51.2	35
1182→1197	Czochralski Crystal >35 Ω/cm	SiO	56.3	54.4	580	569	50.3	46.0	16
1198→1214	Czochralski Crystal >35 Ω/cm	SiO	56.1		580		50.0		17
1215→1233	Float-Zoned Crystal >195 Ω/cm	SiO	55.2	53.4	576	567	49.0	46.1	19
1234→1253	Float-Zoned Crystal >195 Ω/cm	SiO	55.1		575		48.9		20
NP62→NP93	Czochralski 7-14 Ω/cm N/P	CeO_2	58.3	60.2	544	544	51.1	52.3	20

Table VII shows the cell numbers for each type of material and diffusion time, and the quantity shipped against the contract. This group of cells was solder coated. Cells from these runs were placed on environmental test (see Figure 10 for the 150°C data). At room temperature, all the parameters were stable for the time tested (8 weeks).

G. RECOVERY AFTER IRRADIATION

We have selected typical recovery data from several cells made using the evaporated-Li method (Figures 12, 13,14, and 16). The cells were irradiated with $10^{14}/cm^2$ doses of 1-MeV electrons (in 6 minutes) at NASA-Goddard. The unannealed portion of damage evident in each of these curves (even after several days) is very likely due to the lack of Li on the extreme edge of the cell. This

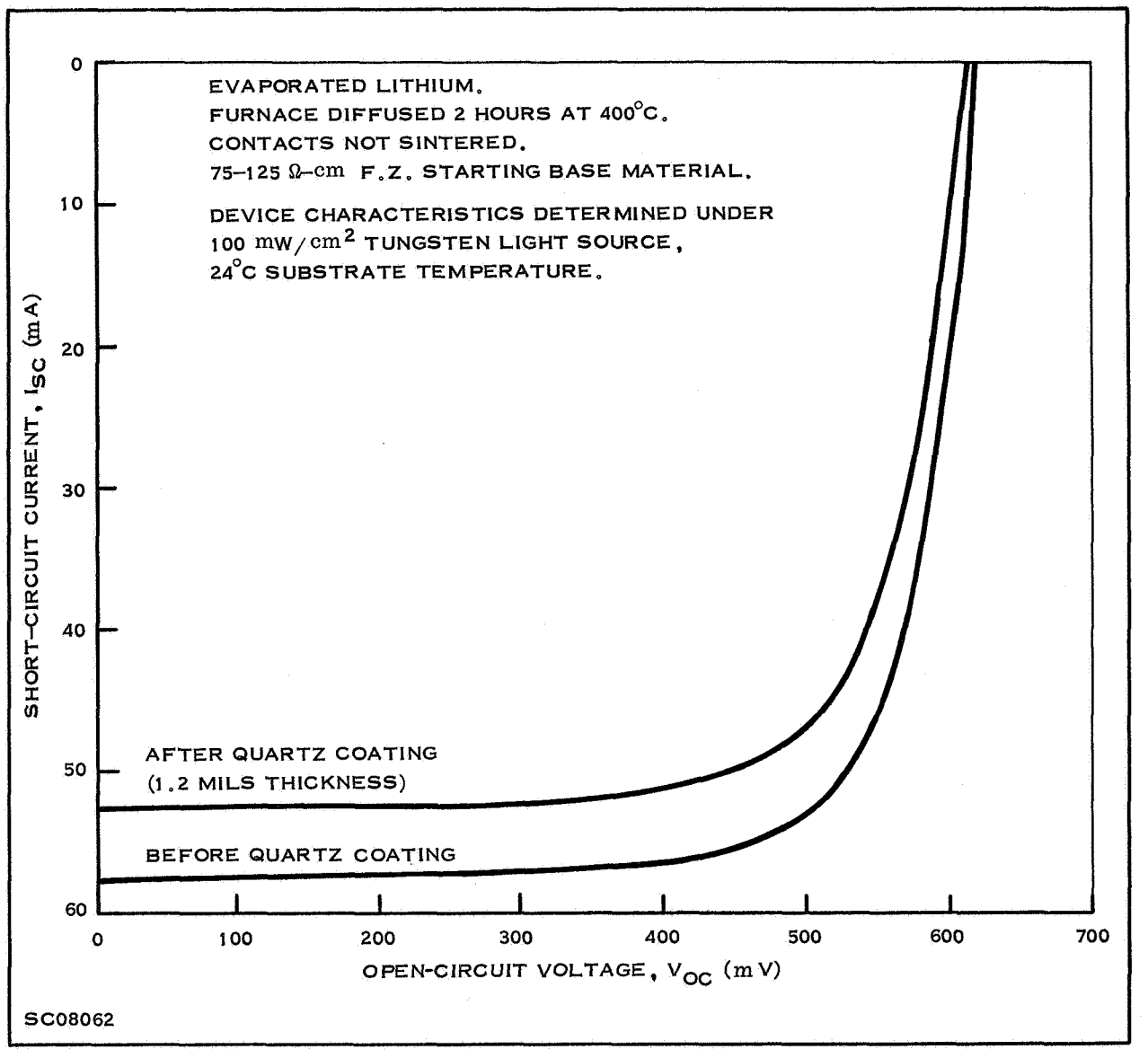

Figure 11. Lithium-Diffused Solar Cell Characteristics Before and After Integral Quartz Coating

Table VI. Effect of Lithium-Diffusion Time

Li Diffusion Time at 400°C in Min	I_{SC} (mA dc)			V_{OC} (mV)			I at 430 mV (mA dc)		
	Fz	Lx	Cz	Fz	Lx	Cz	Fz	Lx	Cz
60	54.1	57.1	55.1	588	592	591	50.2	52.5	51.4
90	54.9	57.8	54.9	587	587	588	50.4	52.9	50.7
120	53.9	57.8	55.0	587	591	585	50.2	54.4	50.5
150	52.0	56.0	53.6	584	594	588	48.2	52.6	49.6

Table VII. Identification for Cells of Table VI

Li Diffusion Time at 400°C in Minutes	Material	Cell No.	Qty.
60	Fz	323-339	13
	Lx	340-353	11
	Cz	354-366	13
90	Fz	367-384	15
	Lx	385-399	13
	Cz	400-418	19
120	Fz	419-436	12
	Lx	437-451	13
	Cz	452-469	17
150	Fz	470-488	16
	Lx	489-503	14
	Cz	504-522	19
		TOTAL	175

point was discussed in Section II.A.1.a. In support of this are the recovery data of cells diffused for 3.8 hours at 400°C, shown in Figure 13. The expected lateral spreading of 19 mils (Table I) is almost enough to cover the cell area and this cell recovered almost completely, though some damage is still unannealed. The Li evaporation for these cells was performed using a mask which left uncoated 20 mils on the edge of the cell. Except for cell T1, the cells were diffused for 2 hours at 400°C. This should result in about 15 mils of lateral spreading (see Table I).

Note also the rapid recovery of cell T1 compared to the others. This is probably due to the larger amount of Li in the junction region. However, at longer times the cell begins to degrade again. This "redegradation" phenomenon is apparently associated with heavy Li concentration ($>$ 5 by $10^{16}/cm^3$) in the vicinity of the junction.

The recovery properties of the Lopex cell T119, shown in Figure 14, are also of considerable interest. First note the large amount of persistent damage (unrecovered efficiency) after 5 hours. This is very likely due to the edge effect mentioned above. After about one day the short-circuit current, i_{SC}, of cell T119 begins to degrade but the open-circuit voltage continues to recover. This redegradation effect is very sporadic from cell to cell and from lot to lot. For example, on an early set of cells all the Lopex cells redegraded, and only a few of the float-zoned cells did so.[4] We now believe that redegradation is due mainly to a heavy Li concentration near the edge of the cell, especially if the cell blank is thinner near the edges. Using the data of Figure 1 along with a measured profile of a chemically polished cell blank, we have constructed a contour map of the Li concentration near the edge of a 13-mil blank. This is shown in Figure 15 along with an estimate of the Li concentration at the P^+N junction in the same vicinity. The high concentration ($>$ $10^{17}cm^{-3}$) in the outer 70 mils suggests the possibility that precipitation (perhaps radiation

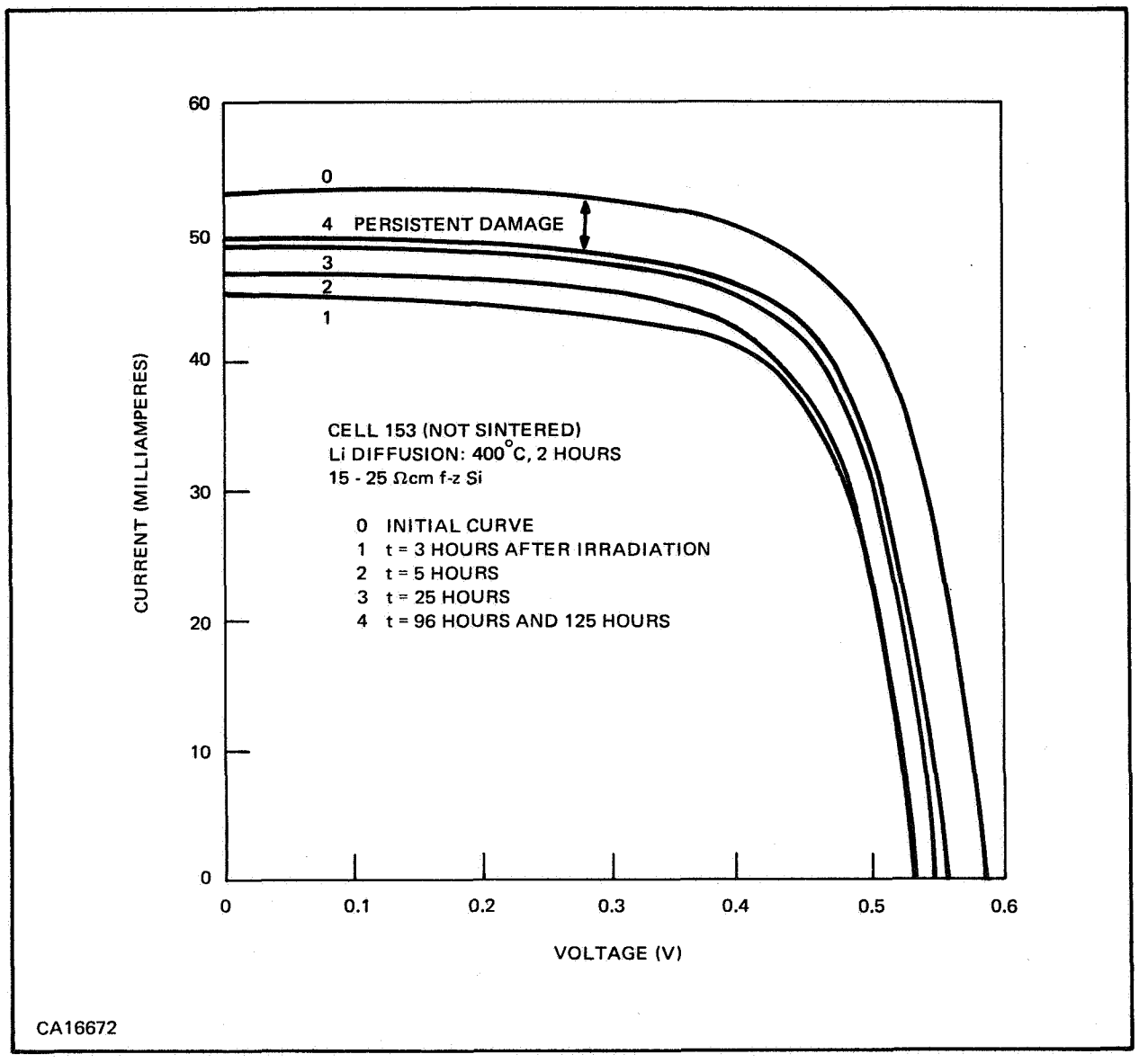

Figure 12. Normal Recovery After Electron Irradiation

induced) may be significant in this region. Furthermore, the variation in edge thickness between lots and cells is expected to be quite large. This leads to wide variations in Li concentration at the junction.

Lithium cells also were fabricated from Czochralski starting material. These contained oxygen in the 10^{17} to $10^{18}/cm^3$ range, which was expected to slow the lithium diffusion considerably.[11] This was indeed the case, as seen in Figure 16. The rate of recovery shown is probably adequate to anneal electron damage as it occurs in many space applications. In addition the oxygen-lithium pairing may hinder the precipitation process, which might eventually degrade the cell. However, this will have to be demonstrated.

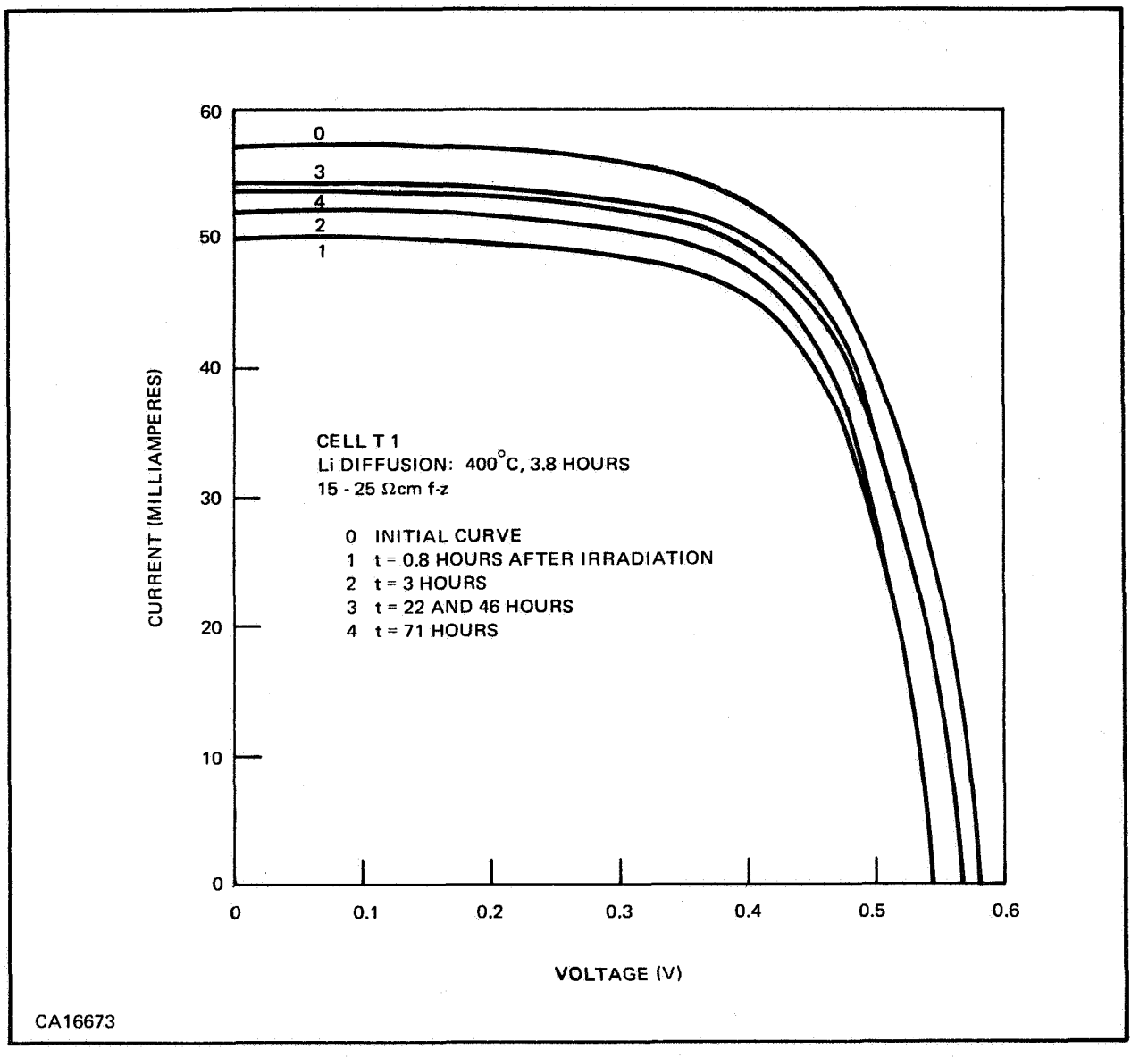

Figure 13. Recovery After Electron Irradiation Showing Rapid Recovery of Heavily Lithium-Doped Cell

H. OXYGEN ANALYSIS

A report has been received from the Texas A & M Activation Analysis Laboratory on the silicon samples provided. This is reproduced below. The work was done by Dr. E. A. Schweikert. To quote from a letter received from Dr. Schweikert:

"It can be deduced from the following experimental results that the sensitivity limit for oxygen obtained for He-3 activation (0.4 ppm or about $2 \times 10^{15}/cm^3$) could easily be improved a factor of 10, thus allowing one to detect about $2 \times 10^{15}/cm^3$ of oxygen in Si. It should be

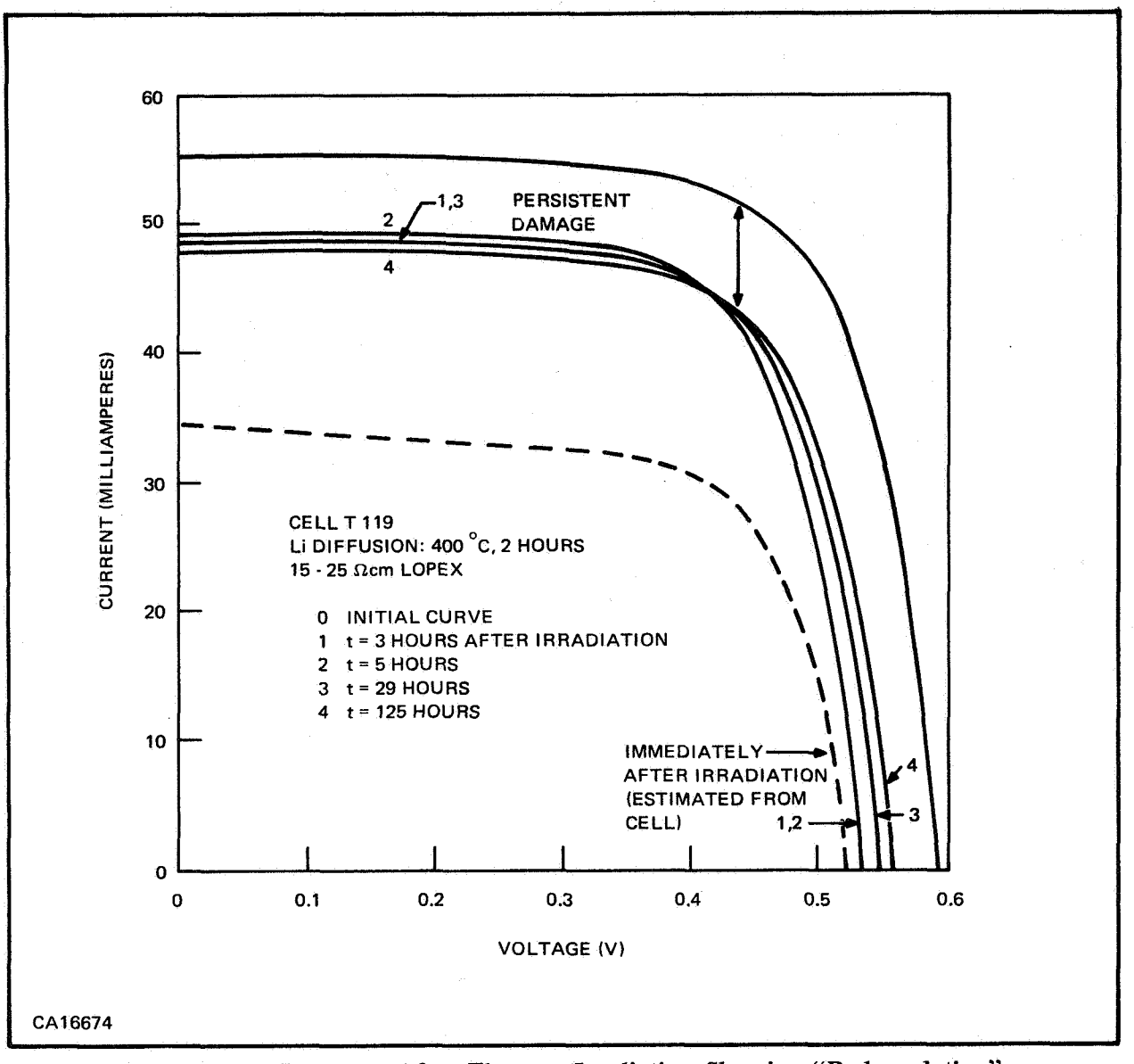

Figure 14. Recovery After Electron Irradiation Showing "Redegradation" of Short-Circuit Current

emphasized that for these determinations the samples were etched after irradiation in order to remove the superficial layers, thus avoiding any possible interfering contribution from surface pollution." Text of the laboratory report is as follows:

Feasibility Study on the Determination of Oxygen

in Silicon Using High-Energy Protons

and He-3 Particles

Results Si Pulled S-9238

First determination after irradiation in protons of 10.40 MeV for 15 min, beam current of 5 μA. Etching after irradiation: 0.0012 inch.

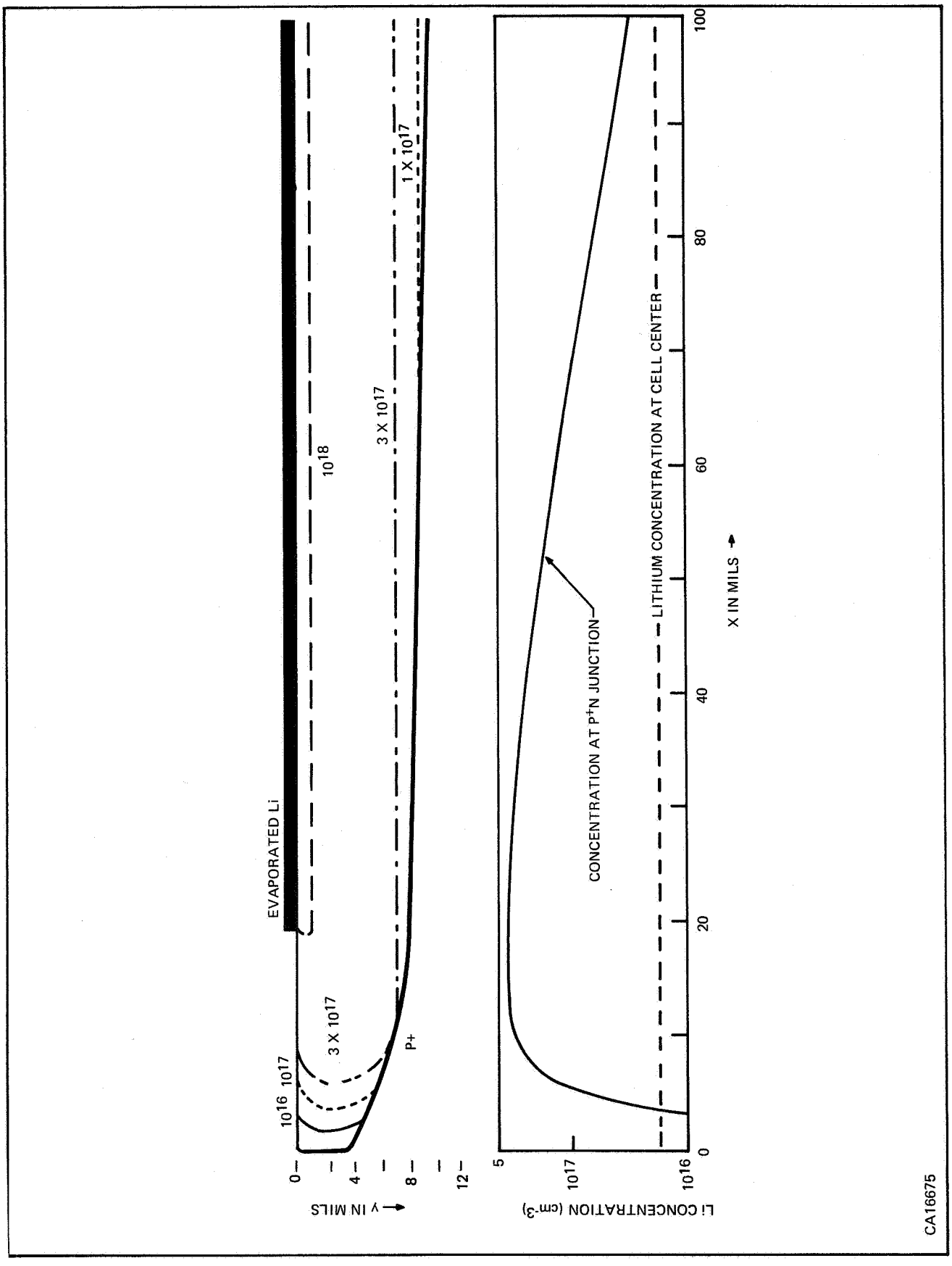

Figure 15. Expected Lithium Concentration Near Cell Edge (Chemically Polished Blank)

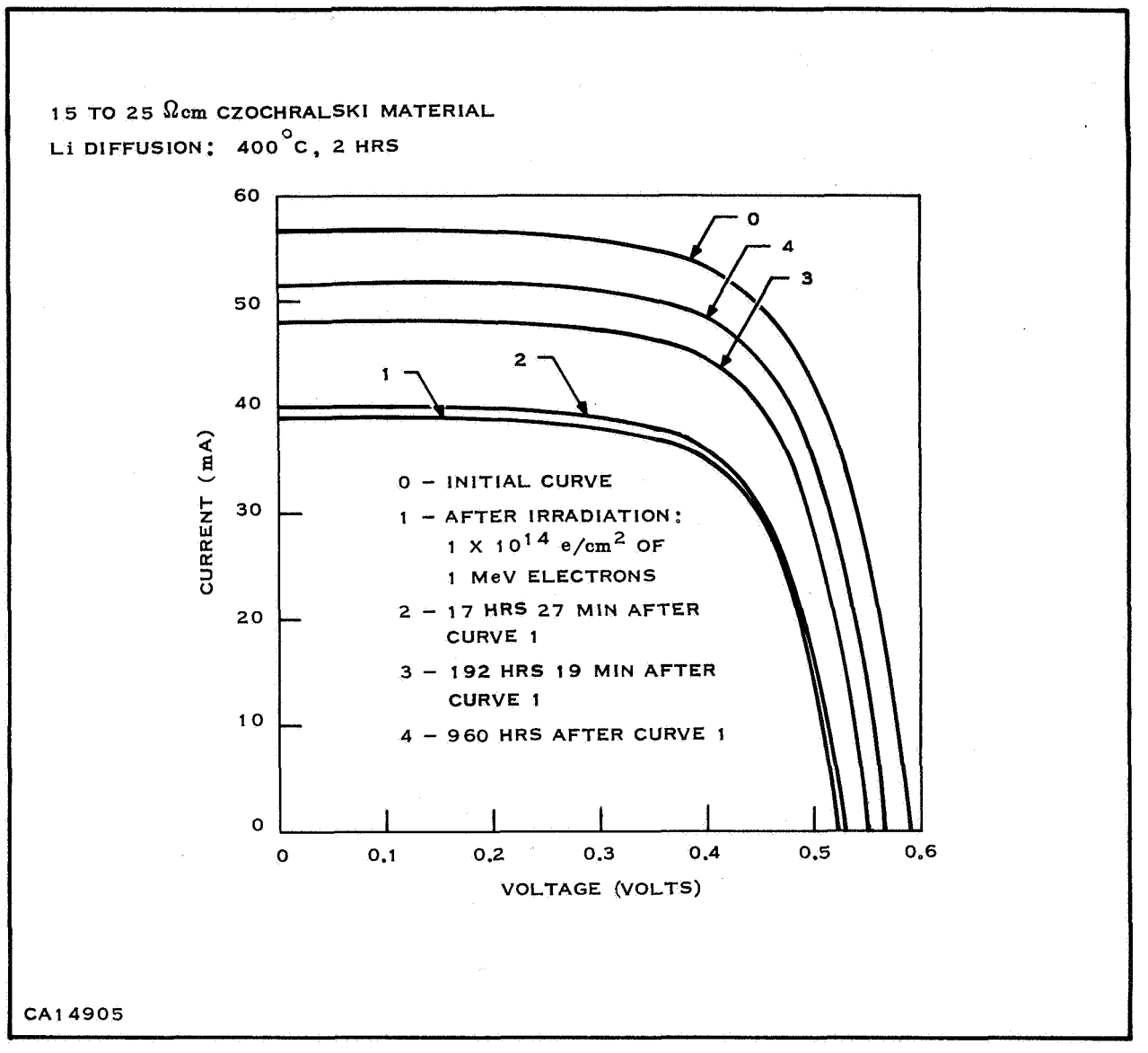

Figure 16. Recovery After Electron Irradiation of Czochralski-Base Cell

Limit of detection for oxygen in this irradiation: 3 ppm. Oxygen content: 15 to 20 ppm.

Second determination after irradiation in He-3 particles of 15.40 MeV for 20 min, 2 μA beam current etching after irradiation: 0.0007 inch. Considering the first etching done in the previous irradiation with protons, this determination applies to a sample slice 0.0019 inch inside from the initial surface. Limit of detection for oxygen in this irradiation: ~ 1 ppm.

Oxygen content: 12 to 16 ppm.

Si FZ S-9582 C
Irradiation in protons of 10.40 MeV for 53 min. 5 μA beam current.

Etching after irradiation: 0.001 inch.

Limit of detection for oxygen in this irradiation: $\sim$ 0.5 ppm.

Oxygen content (not detected): $\leqslant$ 0.5 ppm.

Si FZ S-9582 C
Irradiation in He-3 particles of 15.40 MeV for 30 min, 3 μA beam current.

Etching after irradiation: 0.0015 inch.

Limit of detection for oxygen in this irradiation: $\sim$ 0.4 ppm.

Oxygen content (not detected): $\leqslant$ 0.4 ppm.

Comments

1) For different reasons (limited irradiation time on the cyclotron, lack of counting equipment, failures of the cyclotron, pollution of the single available detection system by another experimenter, etc.), only a very limited number of irradiations could be performed.

2) The experimental arrangement was the following (see Figure 17): a standard (SiO_2) was irradiated under given conditions together with a thin mica foil (6 μ thick, containing 0.25 mg O_2); then a sample was irradiated under the same conditions, together with a mica foil. The activities of the mica foils were compared to check whether the irradiation conditions were similar for both irradiations; activities obtained for the standard were then compared with those of the standard. (Ranges for protons and He-3 particles of different energies in silicon are given in Figure 18.)

3) A. *Results for Si pulled S-9238:* A first determination using protons gave 15 to 20 ppm; a second determination further inside the same sample using He-3 particles gave 12 to 16 ppm.

The decay curve obtained for the activity induced by proton activation was not a pure ^{18}F decay [^{18}F produced by $^{18}O(p,n)^{18}F$], but a complex curve indicated the presence of other impurities (C, N, B ?). The determination of oxygen was therefore less accurate. Limitations in the counting possibilities didn't allow following the decay sufficiently long to see if some very long-lived activity due to other impurities would be present.

The result obtained for the second irradiation using He-3 particles seems to be more accurate. The decay curve obtained is virtually pure showing the decay of ^{18}F produced by $^{16}O(^3He,p)^{18}F$.

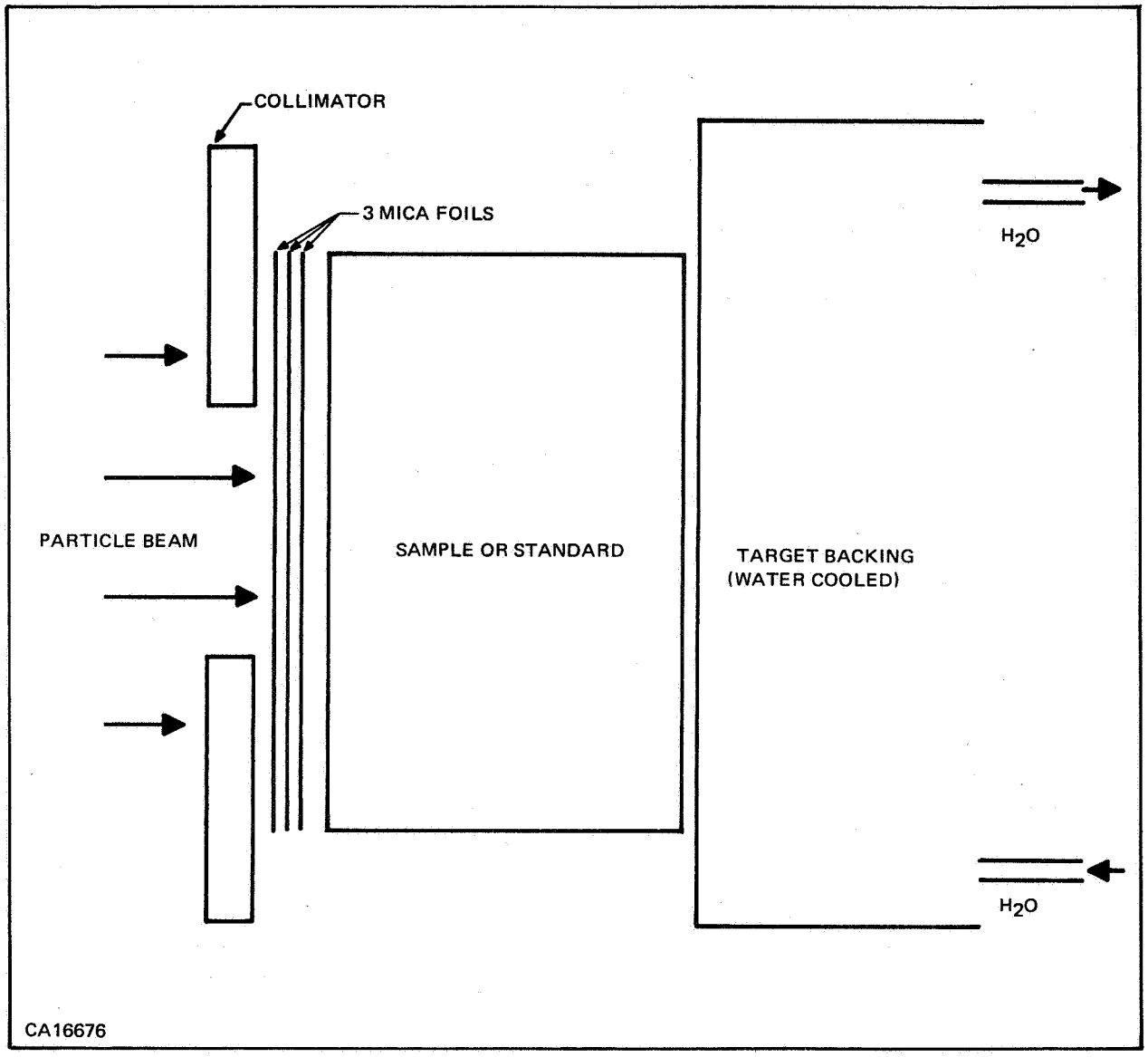

Figure 17. Cyclotron Bombardment Setup

B. The FZ silicon samples (FZ 9582-C) must be of a very-high-purity grade as no activity due to an impurity could be detected (only an almost pure decay curve due to the short-lived activity induced on silicon itself). The result given for activation using He-3 particles ($\leqslant$ 0.4 ppm or $\leqslant 2 \times 10^{16}$ atoms O/cc Si) is obtained from an experiment for which a good number of counting measurements could be taken. The accuracy should therefore be acceptable. For the results obtained with protons ($\leqslant$ 0.5 ppm) less experimental data have been obtained.

4) The sensitivities obtained for the determination of oxygen in silicon were very limited for these irradiations. However, it is obvious that the sensitivity could easily be increased by a factor of 10; for instance, He-3 irradiation of 100 min, 10 μA beam current and better counting conditions, instead of 30 min, 3 μA.

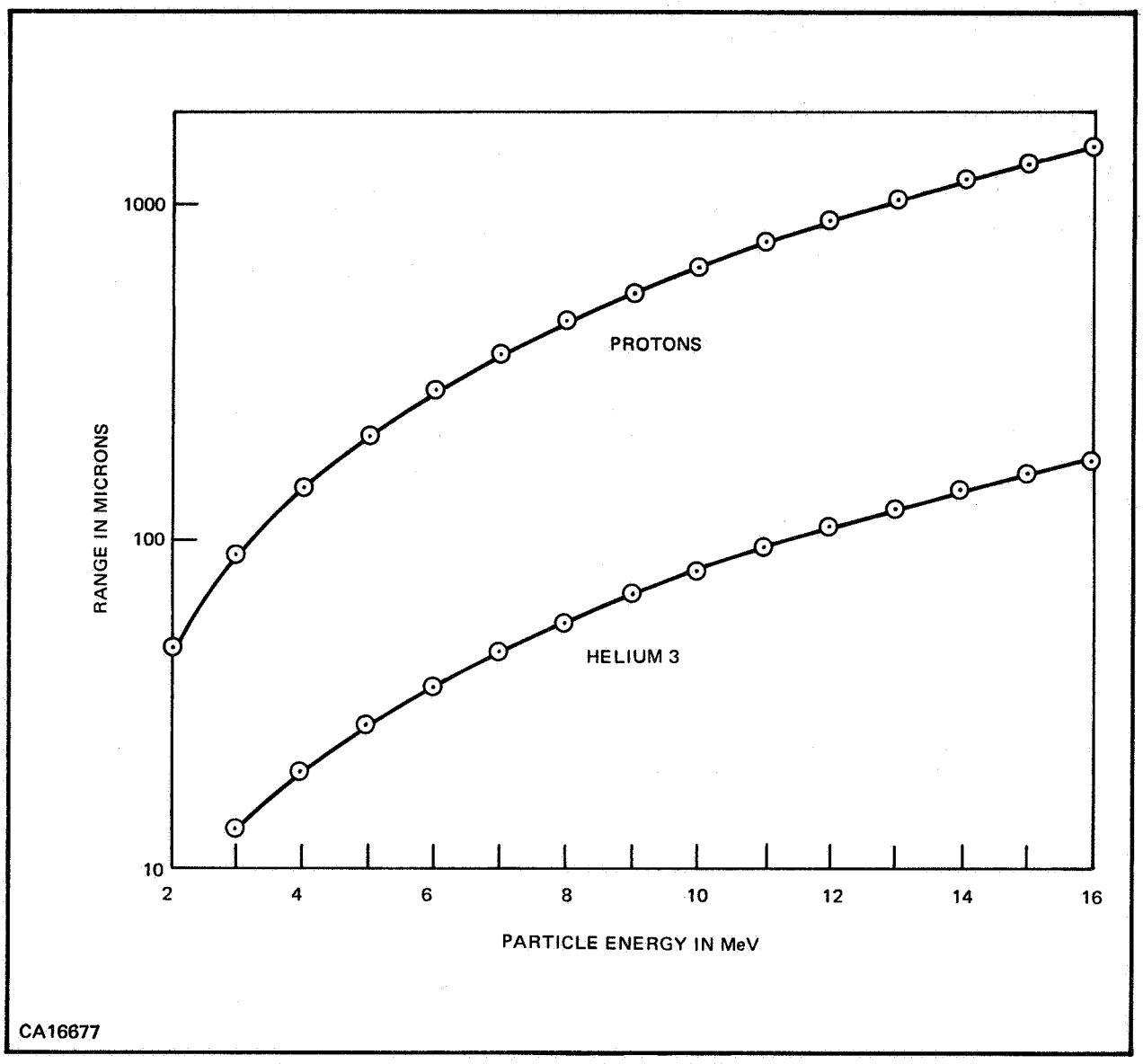

Figure 18. Range for Protons and Helium 3 Energies in Silicon

I. EFFECT OF PROTON BOMBARDMENT ON SILICON SOLAR CELLS SPUTTERED WITH INSULATOR FILMS

Silicon solar cells of both N/P and P/N (lithium-diffused) types were fabricated with integral protective covers. Three test matrices, each comprising covered, integral, and conventional covered cells, were irradiated with 440-keV protons. The source consisted of Southern Methodist University PN400 Van de Graaff accelerator and analyzing magnet. A rotating substrate holder was used during the irradiations to assure uniform flux distribution on all test cells.

The photovoltaic output characteristics of the cells were plotted under a tungsten light source before and after irradiation. The unprotected N/P cells degraded from approximately 12.5 percent conversion efficiency to 0.7 percent after a total proton integrated flux of 1 by 10^{15} p · cm^{-2}. The

N/P cells with 6-mil integral covers and with 6-mil conventional covers decreased approximately 0.6 and 1.5 percent, respectively, in conversion efficiency after 1 by 10^{15} p · cm^{-2}. In the same proton irradiations the unprotected P/N (lithium-diffused) cells were almost completely degraded (final efficiency $\approx$ 0.1 percent), while the 1-mil integrally covered cells of the same type experienced an average of 1.1 percent loss in efficiency.

The degradation in the integrally coated cells was attributed to the damage in small unprotected areas on either end of the cells. The degradation in the conventionally covered cells was primarily caused by a decrease of approximately 6.5 percent in the transmittance of the coverslide in the range of 0.4 to 1.2 microns. The integral coverslides decreased approximately 1 percent in transmittance under the same conditions.

Figures 19 and 20 show the output characteristics of lithium-diffused cells with and without 1-mil integral protective shields, respectively, after total proton fluxes of 7.5 by 10^{11}, 9.3 by 10^{12}, 1 by 10^{14}, and 9.6 by 10^{14} p · cm^{-2} of 440-keV protons. The curves were plotted under a 100 mW/cm^2 tungsten light source calibrated with an N/P Table Mountain standard cell.

The flux from these experiments was on the order of 1 by 10^{11} p · cm^{-2} · sec^{-1}, which is much larger than would be encountered in near-earth orbit space missions. Under the most severe orbit conditions the cells would encounter a maximum of 2 by 10^8 p · cm^{-2} · sec^{-1} protons of 0.1 to 4 MeV energy.[13] However, it was impossible to stabilize the Van de Graaff at a beam current that would yield these rates. The conditions selected yielded the optimum length of time for the test run for stable test conditions. The tests were intended to overstress the integral coatings to assure they would be applicable to lower-stress space-flight missions.

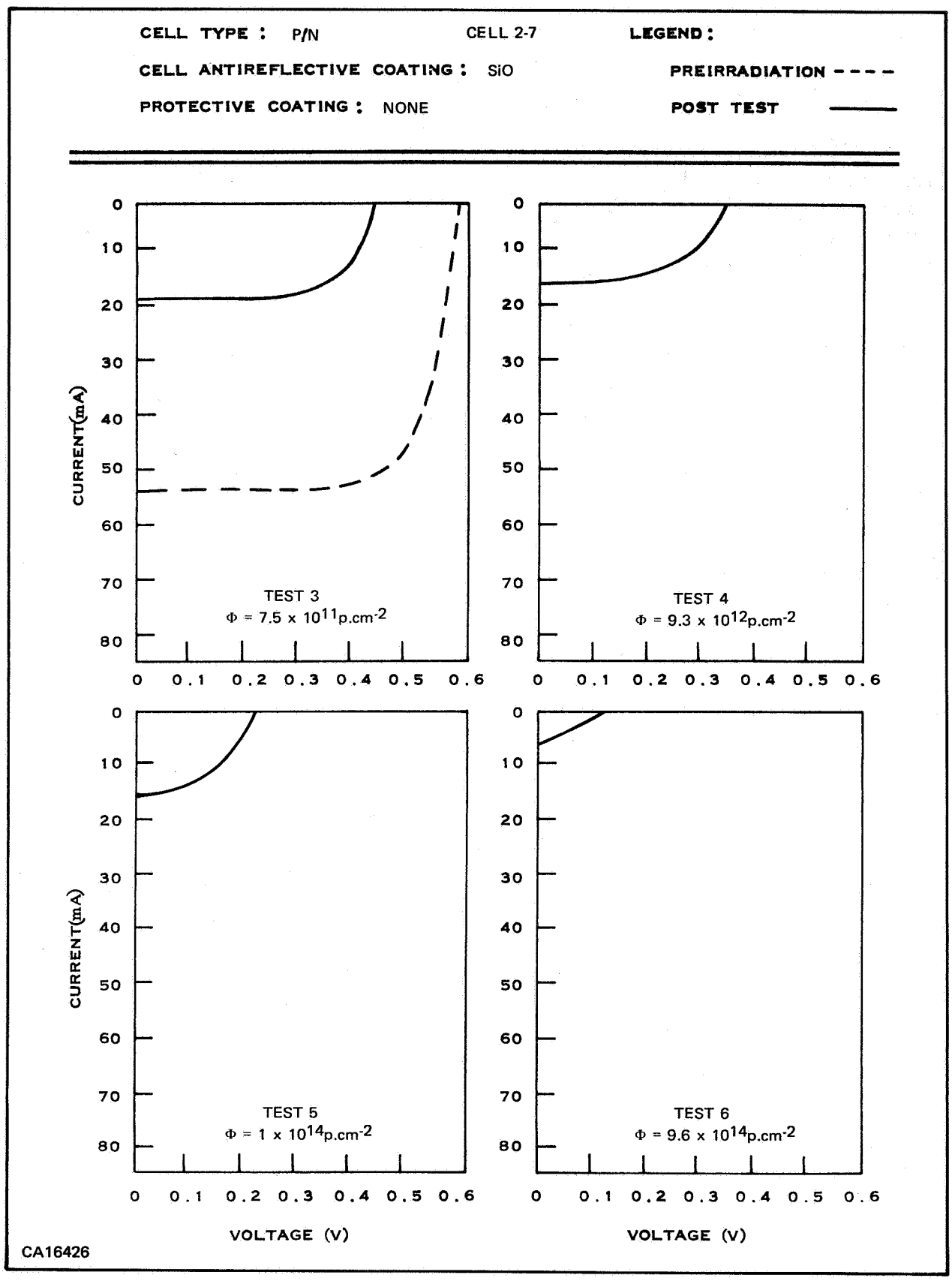

Figure 19. 440-keV Proton Damage to Unprotected Lithium Cells

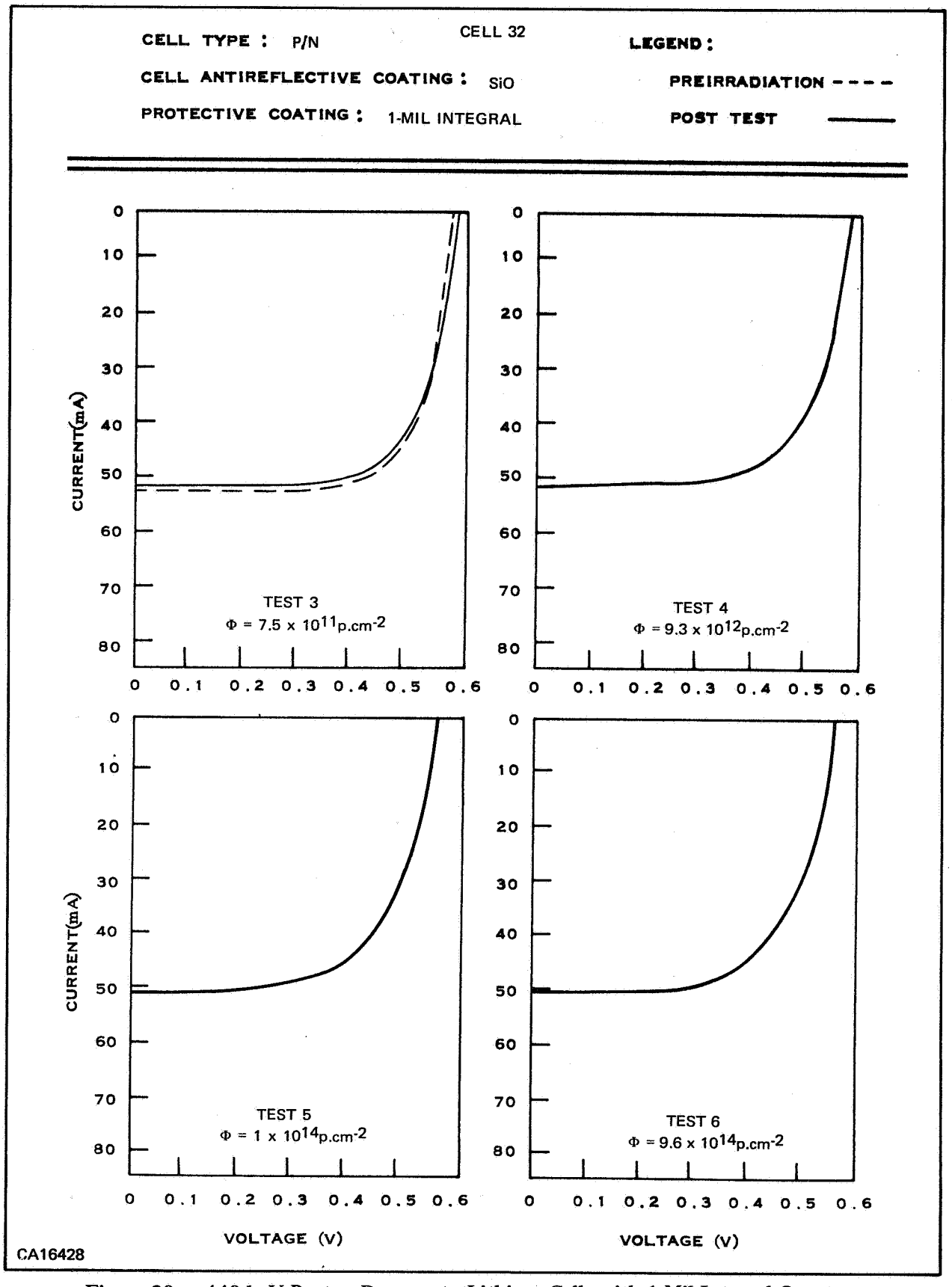

Figure 20. 440-keV Proton Damage to Lithium Cells with 1-Mil Integral Quartz

SECTION III

SUMMARY

During the course of this work we have investigated many of the factors involved in the manufacture of a high-quality lithium-doped silicon solar cell. The significant points are listed as follows:

1) Evaporated-lithium and paint-on techniques give similar results, but the evaporation process yields more consistent cell properties.

2) Penetration depth of the lithium, when diffused from one side of a silicon slice using either of the above methods at 325°C and 400°C, was determined.

3) Magnitude of the lateral spreading of the lithium in the silicon from the edge of a lithium film was determined.

4) A vapor diffusion process, using a tin:lithium-alloy source, was employed to make prototype cells.

5) The boron-diffused layer profile was determined by sectioning and incremental sheet-resistance methods.

6) Sheet resistance of the boron-diffused region increased significantly during the lithium-vapor diffusion process.

7) Lithium easily penetrates an oxide film.

8) The minority carrier lifetime of lithium-diffused silicon at a given concentration is similar to that of N-type silicon doped with antimony or arsenic.

9) Isothermal annealing of lithium-diffused silicon Hall bars at 200°C causes the average resistivity to double in 30 hours.

10) Isochronal annealing of Hall-bar specimens shows that about 20 minutes at 500°C is adequate to remove almost all the lithium from a 14-mil-thick slab.

11) Lithium-diffused solar cells were heated at 250°C and 150°C. The efficiency of these cells decreased to 90 percent of their initial values in 20 and 800 hours, respectively.

12) Numbers 9, 10, and 11 can all be explained as being simple out-diffusion of the lithium to the surface. Precipitation is apparently not involved at these lithium concentrations ($\leqslant$ 2 by $10^{17}/cm^3$).

13) On the basis of an out-diffusion model, the Lopex and float-zoned-based lithium cells should have a storage life of 200 years at 27°C (ignoring radiation and other effects).

14) A significant concentration of donors of unknown origin is released at about 250°C during isochronal annealing of lithium-diffused silicon.

15) Integral quartz protective shields were successfully applied to lithium-diffused cells with both SiO and CeO_2coatings.

16) The solar-cell electrical parameters are found to be relatively independent of the lithium diffusion time in the 1.0-to-2.5-hour range at 400°C.

17) Most of the cells, after receiving a dose of high-energy electrons, show persistent damage that is not annealed by the lithium process. This is explained as being due to the extreme edges of the cell (outer 15 mils) not containing lithium.

18) Some of the cells recover most of their efficiency in the first two days after irradiation and then begin to degrade again. This redegradation process is evidently associated with high lithium concentration in the vicinity of the P^+N junction.

19) The expected lithium-concentration at the P^+N junction for a typical lithium-diffused cell suggests that the lithium concentration in a zone just inside the outer edge may be 20 times higher than in the central area of the cell.

20) The uncontrolled thickness variations in the outer 100 mils of chemically polished cell blanks are probably responsible for the irreproducibility of the redegradation process.

21) Lithium-diffused cells containing oxygen also recover from high-energy-electron damage, but at a much slower rate.

22) Solar cells of both N/P and P/N (lithium-diffused) were tested for the effect of 440-keV proton bombardment.

23) Unprotected N/P cells degraded from 12.5 percent to 0.7 percent conversion efficiency (AMI) after receiving a fluence of $10^{15}/cm^2$.

24) Unprotected lithium-diffused P/N cells degraded to 0.1 percent after the same dosage.

25) Integral coating of both types of cells with either 1.0 or 6.0 mils of quartz was successful in protecting the cells against these protons.

SECTION IV

REFERENCES

1. Wysocki, J. J., Rappaport, P., Davison, E., and Hand, R., *Appl. Phys. Letters,* 9, 44 (1966).

2. Reiss, H., and Fuller, C. S., *Trans. AIME, J. Metal, 206* p. 276 (1956).

3. Fuller, C. S., and Wolfstirn, K. B., *J. Appl. Phys.,* 33, p. 2507 (1962).

4. Kendall, D. L., and Vineyard, R. A., Conference Record of Sixth Photovoltaics Specialist Conference, Vol. III p. 166 (March 1967).

5. Reiss, H., Fuller, C. S., and Morin, F. J., *BSTJ,* 35 p. 535 (1956).

6. Moi, M. E., *Electrochemical Technology,* 5, p. 551 (1967).

7. Horak, J. B., AF Cambridge Contract F 19628-67-0043 Project, No. 4608.

8. Bergmann, F., Fritzsche, C., Riccius, H. D., *Telefunken–Zeitung* 37, p. 186 (1964).

9. Beck, J. W., *J. Appl. Phys.*, 33, p. 2391 (1962).

10. Fuller, C. S., and Logan, R. A., *J. Appl. Phys.*, 28, p. 1427 (1957).

11. Pell, E. M., Solid State Physics, Electronics Telecommuns., *Proc. Intern. Conf. Brussels*, 1958, 1, p. 261 (1960).

12. Vineyard, R. A., Thesis, Southern Methodist University (1968).

13. Vette, J. J., reference 4, page 13.